Environmental factors have a greater influence on photosynthetic capacity in C_4 plants than C_4 biochemical subtypes or growth forms

Yuzhen Fan[1]*, Daniel W. A. Noble[2], Belinda E. Medlyn[3], Russell K. Monson[4], Rowan F. Sage[5], Nicholas G. Smith[6], Elizabeth A. Ainsworth[7,8,9], Florian A. Busch[10], Florence R. Danila[1], Maria Ermakova[11], Patrick Friesen[12], Robert T. Furbank[1], Shu Han Gan[13], Oula Ghannoum[3], Daniel M. Griffith[14], Lianhong Gu[15], Vinod Jacob[3], Jürgen Knauer[16], Andrew D. B. Leakey[7,8,9], Shuai Li[7,8,17], Danica L. Lombardozzi[18,19], Martha Ludwig[20], Varsha S. Pathare[9], Murilo M. Peixoto[21,22], Karine Prado[23], Balasaheb V. Sonawane[9], Christopher J. Still[24], Susanne von Caemmerer[1], Russell Woodford[11], Danielle A. Way[1,25,26]*

*Authors for correspondence

Yuzhen Fan (yuzhen.fan@anu.edu.au)

Danielle A. Way (danielle.way@anu.edu.au)

Number of Figures: 7 (+7 in Supplementary)

Number of Tables: 1 (+1 in Supplementary)

Number of References: 145

Number of Pages (main text): 17

Word count (incl. in-text citations): Total (7,489), Abstract (196), Introduction (1,819), Materials and Methods (1,934), Results (1,189), Discussion (2,547)

Running title: A data synthesis of C_4 A/C_i curves

Affiliation

[1]Division of Plant Sciences, Research School of Biology, The Australian National University, Canberra, ACT 2601, Australia
[2]Division of Ecology and Evolution, Research School of Biology, The Australian National University, Canberra, ACT 2601, Australia
[3]Hawkesbury Institute for the Environment, Western Sydney University, Penrith, NSW 2751, Australia
[4]Department of Ecology and Evolutionary Biology, University of Colorado, Boulder, CO 80309, USA
[5]Department of Ecology and Evolutionary Biology, University of Toronto, Toronto, ON M5R3C5, Canada
[6]Department of Biological Sciences, Texas Tech University, Lubbock, TX 79409, USA
[7]Center for Advanced Bioenergy and Bioproducts Innovation, University of Illinois at Urbana-Champaign, Urbana, IL 61801, USA
[8]Carl R. Woese Institute for Genomic Biology, University of Illinois at Urbana-Champaign, Urbana, IL 61801, USA
[9]Departments of Plant Biology and Crop Sciences, University of Illinois Urbana Champaign, Urbana, IL 61801, USA
[10]School of Biosciences and Birmingham Institute of Forest Research, University of Birmingham, Birmingham B15 2TT, UK
[11]School of Biological Sciences, Monash University, Melbourne, VIC 3800, Australia
[12]BioChambers, Winnipeg, MB R2W 3A8, Canada
[13]Department of Ecology, Evolution & Environmental Biology, Columbia University, New York, NY 10027, USA
[14]Forest Ecosystems and Society, Oregon State University, Corvallis, OR 97331, USA
[15]Environmental Sciences Division and Climate Change Science Institute, Oak Ridge National Laboratory, Oak Ridge, TN 37831, USA
[16]School of Life Sciences, Faculty of Science, University of Technology Sydney, Ultimo, NSW 2007, Australia
[17]Guangdong Provincial Key Laboratory of Applied Botany, South China Botanical Garden, Chinese Academy of Sciences, Guangzhou, Guangdong 510650, China
[18]Department of Ecosystem Science & Sustainability, Colorado State University, Fort Collins, CO 80523, USA

[19]Climate and Global Dynamics Laboratory, National Center for Atmospheric Research, Boulder, CO 80305, USA
[20]School of Molecular Sciences, University of Western Australia, Perth, WA 6009, Australia
[21]School of Biological Sciences, Washington State University, Pullman, WA 99164, USA
[22]Universidade Federal de Goiás, Programa de Pós-graduação em Biodiversidade Vegetal, Instituto de Ciências Biológicas, Goiânia, GO 74690-900, Brazil.
[23]Plant Resilience Institute, Department of Biochemistry and Molecular Biology, Michigan State University, East Lansing, MI 48823, USA
[24]Department of Forest Ecosystems and Society, Oregon State University, Corvallis, OR 97331, USA
[25]Department of Biology, The University of Western Ontario, London, ON N6A 3K7, Canada
[26]Nicholas School of the Environment, Duke University, Durham, NC 27708, USA

ORCID

Yuzhen Fan: 0000-0003-1857-9244
Daniel W. A. Noble: 0000-0001-9460-8743
Belinda E. Medlyn: 0000-0001-5728-9827
Russell K. Monson: 0000-0002-7671-4371
Rowan F. Sage: 0000-0001-6183-9246
Nicholas G. Smith: 0000-0001-7048-4387
Elizabeth A. Ainsworth: 0000-0002-3199-8999
Florian A. Busch: 0000-0001-6912-0156
Florence R. Danila: 0000-0002-7352-3852
Maria Ermakova: 0000-0001-8466-4186
Patrick Friesen: 0000-0002-1027-4502
Robert T. Furbank: 0000-0001-8700-6613
Shu Han Gan: 0000-0002-8699-3669
Oula Ghannoum: 0000-0002-1341-0741
Daniel M. Griffith: 0000-0001-7463-4004
Lianhong Gu: 0000-0001-5756-8738
Vinod Jacob: 0000-0002-6627-5993

Jürgen Knauer: 0000-0002-4947-7067
Andrew D. B. Leakey: 0000-0001-6251-024X
Shuai Li: 0000-0003-2545-7763
Danica L. Lombardozzi: 0000-0003-3557-7929
Martha Ludwig: 0000-0002-0324-7602
Varsha S. Pathare: 0000-0001-6220-7531
Murilo M. Peixoto: 0000-0002-6242-6870
Karine Prado: 0000-0002-0502-0380
Balasaheb V. Sonawane: 0000-0001-6539-5179
Christopher J. Still: 0000-0002-8295-4494
Susanne von Caemmerer: 0000-0002-8366-2071
Russell Woodford: 0000-0002-6766-2274
Danielle A. Way: 0000-0003-4801-5319

Abstract

- Our understanding of how photosynthesis varies among C_4 species and across different growth and measurement conditions remains limited.
- We collated 1,696 CO_2 response curves of net CO_2 assimilation rate (A/C_i curves) from C_4 species grown and measured at various environmental conditions and used these data to estimate the apparent maximum carboxylation activity of phosphoenolpyruvate carboxylase (V_{pmaxA}) and CO_2-saturated net photosynthetic rate (A_{max}), two key parameters describing C_4 photosynthetic capacity. We examined how V_{pmaxA} and A_{max} vary with species-specific traits, growth and measurement conditions.
- We show that V_{pmaxA} and A_{max} do not differ between C_4 biochemical subtypes or growth forms, and highlight that growth temperature and measurement conditions are major factors determining photosynthetic capacity. We found no evidence that common C_4 model species (e.g., maize, sorghum and *Setaria viridis*) differ in photosynthetic capacity from other C_4 species when grown in controlled environments. However, C_4 model species showed up to twice the photosynthetic capacity of other C_4 species when grown in the field.
- Our multivariate model accounts for 47-51% of the variation reported in V_{pmaxA} and A_{max}, and we argue that environmental conditions have a greater influence on C_4 photosynthetic capacity than inherent biochemical subtypes or growth forms.

Keywords

A/C_i curve, A_{max}, C_4 photosynthesis, C_4 subtype, environmental response, photosynthesis modelling, V_{pmax}

Introduction

C_4 photosynthesis evolved at least 66 times in the last 35 Myr in response to inefficiencies in C_3 photosynthesis under hot, arid and low CO_2 environments that promote photorespiration (Sage, 2016). In C_4 plants, a CO_2-concentrating mechanism increases CO_2 concentrations at the site of Rubisco (ribulose-1,5-bisphosphate carboxylase/oxygenase) in bundle sheath cells, resulting in an increase in its carboxylase activity, a reduction in photorespiration, and an increase in photosynthetic efficiency (Hatch, 1987). Compared to their C_3 counterparts, C_4 plants require one-third of the amount of Rubisco to achieve the same or higher rates of net CO_2 uptake, leading to greater nitrogen-use efficiency (Ghannoum *et al.*, 2011). C_4 plants also have higher water-use efficiency because they can maintain a lower stomatal conductance relative to the rate of net photosynthetic CO_2 assimilation (A), which supports greater biomass production when water is limited (Evans & von Caemmerer, 1996; Leegood, 2002; Taylor *et al.*, 2010; Ghannoum *et al.*, 2011). Thus, C_4 plants tend to outperform C_3 plants in hot and dry environments, lending them a competitive advantage in subtropical and semiarid ecosystems. As a result, C_4 plants occupy ~20% of the land surface and contribute up to 23% of global gross primary productivity although they comprise <5% of terrestrial plant species (Still *et al.*, 2003; Luo *et al.*, 2024).

Currently, C_4 global primary productivity is typically estimated in Earth System Models using a simplified mechanistic model that uses parameters reflecting photosynthetic capacity (Still *et al.*, 2019; Griffith *et al.*, 2020). The model and its parameter values are largely derived from data collected on a single species, *Zea mays* (maize) (Collatz *et al.*, 1992). Consequently, the model does not capture substantial variation across C_4 species in the biochemistry underlying CO_2 assimilation (Hatch, 1987), or in their growth forms (Poorter *et al.*, 2009; Liu *et al.*, 2019). The responses of photosynthetic capacity to environmental parameters, such as temperature and irradiance, are also taken from the same study on maize (Collatz *et al.*, 1992). Over the last 30 years, many studies have reported how C_4 photosynthetic parameters vary in response to environmental drivers and described genetic differences within and between species. However, these findings are scattered across publications, except for an analysis by Pignon & Long (2020), and have not been subjected to data synthesis in a manner that could advance the representation of this important plant functional type in Earth System Models.

The most common way to estimate leaf-level photosynthetic capacity is to measure CO_2 response curves of net CO_2 assimilation rate (i.e. A/C_i curves), and assess both the initial slope of the A/C_i curve (a parameter closely related to the apparent maximum activity of phosphoenolpyruvate (PEP) carboxylase, V_{pmaxA}) and the horizontal asymptote of the A/C_i curve (i.e. the rate of CO_2-saturated net photosynthesis, termed A_{max}). The initial slope of a C_4 A/C_i curve is generally insensitive to changes in leaf measurement temperatures (T_{leaf}) for plants grown at moderate temperatures (Long & Woolhouse, 1978; Laisk & Edwards, 1997; Sage, 2002), although it can be reduced in plants grown under chilling conditions, possibly reflecting an increase in the activation energy of PEP carboxylase (PEPc) at low temperatures (Pittermann & Sage, 2001; Kubien & Sage, 2004). In contrast, A_{max} increases with increasing T_{leaf} in C_4 plants grown under moderate temperatures (Sage & Kubien, 2007). As with T_{leaf}, the initial slope of a C_4 A/C_i curve remains largely stable when measured at moderate versus high photosynthetic photon flux density (*PPFD*) (e.g. 500 vs. 1,500 μmol photons m^{-2} s^{-1}), suggesting that irradiance does not directly change PEPc kinetics, and PEP regeneration may not be the limiting step of photosynthesis at low C_i (Pengelly *et al.*, 2010). However, A_{max} is sensitive to changes in irradiance and increases when measured under high *PPFD* (Pengelly *et al.*, 2010). This irradiance response of A_{max} may result from the alleviation of chloroplastic electron transport limitation under high *PPFD* (Ermakova *et al.*, 2019, 2023), thereby enhancing energy availability for PEP or RuBP regeneration, leading to higher overall net photosynthesis (von Caemmerer & Furbank, 2016). Taken together, the responses of photosynthetic capacity to measurement conditions are dynamic, with the initial slope of the A/C_i curve tending to be less affected by T_{leaf} and *PPFD* than A_{max}.

C_4 photosynthetic capacity can also be altered by growth temperatures. There is evidence that photosynthetic capacity (particularly A_{max}) is reduced in C_4 plants grown at warm to high temperatures (i.e. 30 to 43°C), as a result of lower Rubisco content and/or activity, NADP-malic enzyme activity, cytochrome *f* content and carbonic anhydrase activity (Pearcy, 1977; Ward, 1987; Dwyer *et al.*, 2007). In contrast, the activity of PEPc (and potentially V_{pmaxA}) may not be affected by high growth temperatures, possibly due to its high thermal stability (Chen *et al.*, 1994; Chinthapalli *et al.*, 2002; Boyd *et al.*, 2015). At low growth temperatures, many chilling-tolerant, cool-adapted C_4 plants show no change in photosynthetic rates or Rubisco concentrations compared to control plants (Pittermann & Sage, 2001; Naidu *et al.*, 2003; Cavaco *et al.*, 2003; Kubien & Sage, 2004), though the content of other photosynthetic enzymes [e.g. pyruvate, phosphate dikinase (PPDK)], can increase (Wang *et al.*, 2008). These findings highlight that while some C_4 plants can adjust their photosynthetic machinery in response to growth temperature, both high and low temperatures can impose biochemical constraints that limit photosynthetic capacity via acclimation and thermal stress.

Given that C_4 photosynthesis is thought to be an evolutionary response to high photorespiratory loads (Sage, 2004), there has been considerable interest in the response of C_4 photosynthesis to variation in CO_2 concentrations. When C_4 plants are grown in controlled environments, A_{max} can increase under sub-ambient CO_2 conditions, reflecting an up-regulation of Rubisco capacity to enhance carbon capture (Ripley *et al.*, 2013; Pinto *et al.*, 2014; Cunniff *et al.*, 2017), but remains largely unchanged under the elevated CO_2 levels projected for the coming century (Leakey, 2009; Heckman *et al.*, 2024). In contrast, while the capacity of PEPc in controlled environment-grown plants can also be increased at glacial CO_2 concentrations, it can be reduced at elevated CO_2 concentrations (Wong, 1979; Ghannoum *et al.*, 2000; Pinto *et al.*, 2014). However, when C_4 plants are grown in the field, changes in growth CO_2 concentrations had little effect on photosynthesis or the activity/capacity of key photosynthetic enzymes including PEPc (Leakey *et al.*, 2006; Leakey, 2009; Markelz *et al.*, 2011). Both sub-ambient and elevated CO_2 concentrations influence stomatal conductance, leading to changes in plant water relations and interactions with drought stress that can be complex in nature and create opportunities for crop improvement (Ghannoum *et al.*, 2000; Markelz *et al.*, 2011; Leakey *et al.*, 2019). Although our understanding of how C_4 plants respond to changes in CO_2 concentration and drought, along with their underlying physiological mechanisms, has advanced in recent decades [e.g. (Tissue *et al.*, 1995; Wang *et al.*, 2020; Ding *et al.*, 2022)], this knowledge has yet to be fully integrated into ecosystem models (Cowling *et al.*, 2007; Still *et al.*, 2019).

There is some evidence suggesting that the response of C_4 photosynthetic capacity to growth environment depends on the biochemistry, life history and plant functional type of the species (e.g. growth form: monocot versus eudicot) (Liu *et al.*, 2019). Based on the decarboxylases involved, the C_4 photosynthetic pathway can be categorised into three classical biochemical subtypes: NADP-dependent malic enzyme (NADP-ME subtype), NAD-dependent malic enzyme (NAD-ME subtype) and PEP-carboxykinase (PCK subtype) (Hatch, 1987; von Caemmerer & Furbank, 2016). Considerable variation in biochemical components (e.g. enzyme abundance) and photosynthetic capacity has been found in C_4 plants of different growth forms within and between C_4 biochemical subtypes. For example, the maximum carboxylation activity of PEPc and Rubisco, A_{max} and leakiness (i.e. the CO_2 fraction that leaks out from bundle sheath cells) responded to a short-term increase in T_{leaf} differently in eight C_4 grasses representing the three C_4 biochemical subtypes (Sonawane *et al.*, 2017). In addition, C_4 annual species have been shown to exhibit a greater sensitivity of the chloroplastic electron transport capacity to T_{leaf} than C_4 perennial species (Smith & Dukes, 2017). These findings suggest that differences in C_4 biochemistry and growth form could play a role in determining photosynthetic responses to environmental conditions.

To understand how C_4 photosynthetic capacity responds to environmental cues—and whether these responses differ systematically among biochemical subtypes and growth forms—data are needed from diverse species grown and measured under contrasting environmental conditions. Unfortunately, while numerous studies have evaluated photosynthetic capacity of C_4 plants under various growth and measurement conditions (reference herein), these data are largely siloed in their separate publications, making it challenging to identify broad patterns in photosynthetic traits across C_4 species. In this study, we used published gas-exchange data to explore the drivers of variation in C_4 photosynthetic capacity. Here, A/C_i curves measured from diverse C_4 species across studies were collated to estimate V_pmaxA and A_max with a widely used C_4 mechanistic model (von Caemmerer & Furbank, 1999; von Caemmerer, 2000, 2021). We assessed how V_pmaxA and A_max are affected by species-specific traits (biochemical subtype and growth form) and environmental parameters (growth and measurement conditions). For growth conditions, we considered growth temperature and growth CO_2 concentration. We also considered growth location (whether plants were grown in outdoor fields or in indoor controlled environments; see Materials and Methods for definitions). Compared to outdoor plants, indoor plants may experience limited growth space and different environments (e.g. fewer pests, relatively steady temperature and light conditions), which can affect overall morphology and physiology (Poorter *et al.*, 2016). For measurement conditions, we were interested in how C_4 photosynthetic capacity varies with measurement T_leaf and *PPFD*. An A/C_i curve should be measured under light-saturating conditions, such that *PPFD* is often not considered a key factor in photosynthetic capacity. However, the *PPFD* required for light saturation of net photosynthesis can vary with growth conditions, and A/C_i curves can also be measured under sub-saturating *PPFD* to address specific research questions [e.g. (Sonawane *et al.*, 2018)].

Using these data, we test the following hypotheses:

(1) V_pmaxA and A_max are positively correlated;

(2) C_4 biochemical subtype and growth form alter V_pmaxA and A_max in a systematic way;

(3) Indoor plants show a higher photosynthetic capacity than their outdoor counterparts due to more optimal growth conditions;

(4) Cool-grown plants have a higher photosynthetic capacity relative to their warm-grown counterparts when measured at a common T_leaf;

(5) A_max increases with increasing T_leaf and measurement *PPFD,* but V_pmaxA does not;

(6) Elevated growth CO_2 concentrations have no effect on photosynthetic capacity in C_4 species.

Lastly, we assess whether the photosynthetic capacity of popular C_4 model species—maize, *Sorghum bicolor* (sorghum), and *Setaria viridis*—the three most abundant species in our dataset, is similar to that of other C_4 species to assess whether data from these three species can be used to represent the broad range of undomesticated C_4 species found in nature. We hypothesise that:

(7) These C_4 model species show higher V_{pmaxA} and A_{max} than other C_4 species in the analysis.

Materials and Methods

Data acquisition

This work was conceived by members of the C_4 Working Group supported by the U.S Geological Survey's Powell Center, with data collaboratively sourced within the group and from researchers closely associated with its members. C_4 A/C_i data were compiled from 52 studies published between 2001 and 2024 (Pittermann & Sage, 2001; Anderson *et al.*, 2001; Cousins & Bloom, 2003; Leakey *et al.*, 2006; Kim *et al.*, 2006; Ripley *et al.*, 2007, 2008, 2010, 2013; Nippert *et al.*, 2007; Kakani *et al.*, 2008a,b; Osborne *et al.*, 2008; Horst *et al.*, 2008; Soares *et al.*, 2008; Cunniff *et al.*, 2008; Carmo-Silva *et al.*, 2008; Mantlana *et al.*, 2008; Pengelly *et al.*, 2010; de Souza, 2011; Soares-Cordeiro *et al.*, 2011; Pinto *et al.*, 2011, 2014; Arena *et al.*, 2011; Wang *et al.*, 2012; Bloom *et al.*, 2012; Sun *et al.*, 2012; Vogan & Sage, 2012; Fay *et al.*, 2012; Feng *et al.*, 2012; Chen *et al.*, 2013; Sage *et al.*, 2013; Oakley *et al.*, 2014; Xu *et al.*, 2014; Bissinger *et al.*, 2014; Friesen *et al.*, 2014; Sharwood *et al.*, 2014; Ge *et al.*, 2014; Głowacka *et al.*, 2015; Sonawane *et al.*, 2017, 2018; Peixoto & Sage, 2017; Smith & Dukes, 2018; Li *et al.*, 2019, 2021, 2022; Khoshravesh *et al.*, 2020; Pathare *et al.*, 2020; Danila *et al.*, 2021; Peixoto *et al.*, 2021; Liu *et al.*, 2023; Gan & Sage, 2024; Ermakova *et al.*, 2024) and five unpublished datasets with permission to use. Together, 1,696 C_4 A/C_i curves for 74 species of 12 plant families from 57 unique studies were included in the analysis. Raw data files (i.e. direct output files from the measuring instrument) were requested from authors where available. In cases where the raw data files were not available, curves were digitised from published figures as per Pignon & Long (2020). The compiled dataset is provided in Supplementary Dataset S1.

A/C_i curve analysis

To fit the curves and estimate parameters, the 1,696 individual A/C_i curves were consolidated into 543 groups. Replicate measurements of the same species and genotype that were measured within five days in a study were considered as one experimental group. This approach allowed us to minimise software crashes due to a lack of model convergence and estimate sampling variance; this grouping approach has been used in other studies (e.g. Wu *et al.*, 2024). The A/C_i data at $C_\mathrm{i} < 100$ μmol mol^{-1} (i.e. the initial slope of the A/C_i curve) were used to estimate V_pmaxA, according to von Caemmerer (2000):

$$A = V_\mathrm{p} - R_\mathrm{m} = \frac{C_\mathrm{i} V_\mathrm{pmaxA}}{C_\mathrm{i} + K_\mathrm{p}} - R_\mathrm{m} \qquad \text{Equation (1)}$$

where A is the net CO_2 assimilation rate (μmol CO_2 m^{-2} s^{-1}), V_p is the rate of PEP carboxylation (μmol CO_2 m^{-2} s^{-1}), C_i is the CO_2 concentration in the intercellular space (μmol mol^{-1} CO_2), K_p is the Michaelis-Menten constant for CO_2 (μbar; converted to concentrations using a solubility for CO_2 of 0.0334 mol bar^{-1} and atmospheric pressure at the measurement site; see von Caemmerer *et al.* (1994)), and R_m is daytime mitochondrial respiration in mesophyll cells (μmol CO_2 m^{-2} s^{-1}). Under low C_i, A is linearly correlated with the maximum PEPc activity in mesophyll cells, given that the leakage of CO_2 from bundle sheath cells is low and is generally ignored (von Caemmerer, 2021). We also assumed that PEP substrate concentrations were saturating under the measurement condition, and A was not limited by PEP regeneration, as required by the C_4 model (von Caemmerer, 2000, 2021). K_p was adjusted to account for variation in T_leaf according to Boyd *et al.* (2015):

$$K_\mathrm{p} = K_\mathrm{p25} \times e^{E_\mathrm{a}(T_\mathrm{leaf} - 25)/(298.15R(T_\mathrm{leaf} + 273.15))} \qquad \text{Equation (2)}$$

where K_p25 is K_p measured at 25°C (assumed to be 80 μbar; Bauwe, 1986; DiMario & Cousins, 2019), E_a is the activation energy of K_p (36.3 kJ mol^{-1}; Boyd *et al.*, 2015), and R is the molar gas constant (0.008314 kJ K^{-1} mol^{-1}). R_m was taken as half the daytime leaf mitochondrial respiration rate (R_day) (μmol CO_2 m^{-2} s^{-1}) (von Caemmerer, 2000). Given that there are few R_day measurements in C_4 plants, R_day was assumed to equal leaf dark respiration such that $R_\mathrm{day} = 1.2$ μmol CO_2 m^{-2} s^{-1} at 25°C (termed as R_day25), according to a data synthesis of dark respiration in 39 C_4 species (Fan *et al.*, 2022). R_day was adjusted for variation in T_leaf using a Q_{10} equation (Atkin & Tjoelker, 2003):

$$R_\mathrm{day} = R_\mathrm{day25} \times Q_{10}^{\frac{T_\mathrm{leaf} - 25}{10}} \qquad \text{Equation (3)}$$

where Q_{10} is 2 (Huntingford *et al.*, 2013).

Although mechanistic models for enzyme- and light-limited C_4 photosynthesis are available, C_4 photosynthesis could be co-limited by Rubisco activity, RuBP regeneration and/or PEP regeneration at high C_i, with all three processes requiring energy from light (von Caemmerer & Furbank, 1999). Thus, as no information was provided on the limitation status of photosynthesis at high C_i by individual studies, we estimated A_{max} using the entire A/C_i curve. The A_{max} was estimated by the horizontal asymptote of a four-parameter non-rectangular hyperbolic function (Leakey *et al.*, 2006; Li *et al.*, 2022):

$$\theta(A + R_{\mathrm{day}})^2 - (\alpha C_{\mathrm{i}} + A_{\mathrm{max}})(A + R_{\mathrm{day}}) + \alpha C_{\mathrm{i}} A_{\mathrm{max}} = 0 \qquad \text{Equation (4)}$$

where θ is the curvature factor of an A/C_i curve (unitless), which was assumed to be 0.7 for C_4 plants (Sonawane *et al.*, 2018; von Caemmerer, 2021), and α is the initial slope of an A/C_i curve (μmol CO_2 m^{-2} s^{-1}). We did not include mesophyll conductance as a term in Eq (4) due to a lack of such data in examined studies. However, by assuming $\theta = 0.7$, we considered a potential drop in the C_i between the intercellular space and the site of Rubisco carboxylation (i.e. bundle sheath cells) (Evans, 1989). All curve fitting was performed using the non-linear least square (nls) function and sampling variances of every fit were extracted using the vcov function in R (version 4.3.2, R Core Team, 2018). The number of individual curves per group (n_{group}, ranging from 1 to 9) was also reported. Sampling variance of parameters (i.e., squared standard error for parameters) was subsequently considered in the statistical models (Nakagawa & Santos, 2012; Noble *et al.*, 2017, 2022).

Data classification and summary

Among the 543 groups, eight groups contained fewer than two data points at low C_i (i.e. < 100 μmol mol^{-1}), while 131 groups contained fewer than two data points at high C_i (i.e. > 500 μmol mol^{-1}). As this lack of data is likely to influence the accuracy of model fitting using these portions of the A/C_i curve, the corresponding estimated V_{pmaxA} and A_{max} values of these groups were discarded. Given that measurements within a single group were made under the same measurement temperature and irradiance, we provided averaged values of T_{leaf} and *PPFD* per group. We further assessed the estimated parameters of each group: if the curve violated the assumption that A is limited by V_{pmaxA} at low C_i (as indicated by V_{pmaxA}-limited photosynthesis being higher than A_{max}-limited photosynthesis at low C_i), this group of A/C_i curves was discarded as per Pignon & Long (2020). This assessment led to 108 additional groups being removed from the final dataset (Supplementary Dataset S2), many of which included plants subjected to severe abiotic stresses such as chilling, drought, and low nutrients.

The remaining measurements were classified according to their C_4 biochemical subtype (NADP-ME, NAD-ME or PCK subtype), growth form (monocot or eudicot) and growth location (indoor or outdoor). Indoor plants refer to those grown in pots within controlled environment chambers or glasshouses. In contrast, outdoor plants are grown directly in the soil or in common gardens without pot restrictions. Experiments conducted at Free-Air Carbon Dioxide Enrichment (FACE) and Lysimeter CO_2 Gradient (LYCOG) facilities are classified as outdoor-grown, as plants in these settings are planted directly in soil. The growth CO_2 concentration was noted, where the ambient CO_2 level was assumed to be 400 ppm if not given by the study, as 400 ppm represents the average atmospheric CO_2 concentration from 2001 to 2024 (Friedlingstein *et al.*, 2025), which covers the period of publications used in this study, though the experiments themselves may have been conducted one or two years earlier. For indoor-grown plants, mean maximum (T_{max}) and minimum (T_{min}) growth temperatures were the set daytime and nighttime temperatures, respectively. We used the reported measurement T_{leaf} in our analyses, rather than normalising to a rate at a set temperature of 25°C, as we did not want to assume that the V_{pmax} and A_{max} of all species and growth environments will have the same sensitivity to short-term changes in T_{leaf}. For outdoor-grown plants, mean T_{max} and T_{min} were the mean maximum and minimum temperatures observed across the experimental periods at the study sites, respectively. Growth *PPFD* was unavailable in most outdoor studies and was therefore excluded from the analysis. We were unable to consider either fertilisation treatment or water status as potential categories for analysis, as low nutrient treatment and/or water-stressed conditions constituted <5% of the data (Fig. 1D & E). A summary of measurements based on plant traits and growth treatments is given in Figure 1.

Across the dataset, maize, sorghum and *Setaria viridis* were the three most commonly measured species, accounting for 18%, 6% and 4% of the total measurements, respectively. Indeed, maize contributed 43% of the outdoor data and played an important role in the growth location category (Fig. S1). This species skewness is later accounted for in the statistical models (see below).

Statistical analysis

To determine how different plant traits and experimental conditions altered V_{pmaxA} and A_{max}, we ran two multivariate linear mixed-effects models with V_{pmaxA} or A_{max} as the dependent variable in each model. These models accounted for the sampling variance of each parameter, with parameters having greater precision being weighted more heavily to overall means. We included three main fixed effect categories in our models: (1) species-specific traits, including C_4 subtype and growth form; (2) environmental growth conditions, such as growth location, temperature and CO_2 concentration; and (3) measurement conditions, such as T_{leaf} and *PPFD*. Given that mean T_{max} and T_{min} were strongly positively correlated with each other (Fig. S2), we used mean T_{max} in the model. A list of fixed effects is given in Table 1.

In addition, we included six *a priori* interaction terms examining the interactive effects of species-specific traits, temperatures and irradiance: C_4 subtype × mean T_{max}, C_4 subtype × T_{leaf}, C_4 subtype × *PPFD*, growth form × mean T_{max}, growth form × T_{leaf}, and growth form × *PPFD*. These terms were designed to test the question of whether the response of C_4 photosynthetic capacity traits to short- and long-term temperatures and measurement irradiance differ among C_4 subtypes or growth forms. We confirmed that our V_{pmaxA} and A_{max} data per C_4 subtypes and growth form were distributed across the entire range of mean T_{max}, T_{leaf} and *PPFD* (Fig. S3), such that any significant interaction terms would not be biased due to separated data distributions. Data distribution with respect to mean T_{max} and T_{leaf} is shown in Figure S4. Random effects included in the models were the different studies (indicated by publications), grouping of the curves (see above section titled *C_4 A/C_i analysis*), and species. Given that C_4 model species (maize, sorghum and *Setaria viridis*) made up a significant proportion of the data, we also conducted a case study examining to what extent the model results obtained from data of all species match with those of the C_4 model species and visualise our results with consideration of C_4 model species (see Results).

The multivariate linear mixed-effects models with restricted maximum likelihood estimation were run using the package metafor version 4.6.0 (Viechtbauer, 2010) and plots were made using the package ggplot2 version 3.5.1 (Wickham, 2016) and orchard version 2.0 (Nakagawa *et al.*, 2021, 2023) on R program version 4.4.1 (R Core Team, 2024). Estimated effects were considered significant if $P < 0.05$ in the models.

Results

Positive correlations between V_{pmaxA} and A_{max}

In general, V_{pmaxA} and A_{max} were correlated with each other in a logarithmic manner ($R^2 = 0.81$; Fig. 2A). We found that for leaves measured at a moderate T_{leaf} (i.e. < 35°C), changes in V_{pmaxA} were tightly coupled with changes in A_{max} in a nearly linear fashion (Fig. 2A). When leaves were measured at a hotter T_{leaf} (i.e. > 35°C), the coupling between V_{pmaxA} and A_{max} broke down, and an increase in V_{pmaxA} was accompanied by a lesser increase in $A_{\max}$. This result was supported by significantly different slopes ($P < 0.001$; standardised major axis analysis) in the linear correlations between V_{pmaxA} and $A_{\max}$ for leaves measured at 25–30°C (slope = 0.49; Fig. 2B), 30–35°C (slope = 0.39; Fig. 2C), and 35–40°C (slope = 0.27; Fig. 2D). Together, these findings highlight that at high $A_{\max}$ (i.e. high C_i), photosynthesis was less dependent on PEP carboxylation, compared to other high-temperature sensitive biochemical processes (e.g. Rubisco carboxylation), or photosynthesis was constrained by increased limitations in light and bundle sheath [CO_2] at high $A_{\max}$ (e.g. affecting RuBP regeneration).

Factors influencing V_{pmaxA} and $A_{\max}$ are mostly environmental

Multivariate linear mixed-effects models highlighted several factors that significantly affected both V_{pmaxA} and $A_{\max}$ (Table 1). C_4 subtype identity and growth form had little influence on values of either V_{pmaxA} or $A_{\max}$ (Fig. 3A-D). Note that the number of studies examining eudicots or PCK-type plants was noticeably lower compared to studies focusing on monocots or NADP-ME plants, respectively. This highlights an urgent need to further investigate photosynthetic characteristics in eudicots and PCK-type plants. There is no evidence that V_{pmaxA} and $A_{\max}$ vary among families or subfamilies ($P = 0.73$ and 0.88 for V_{pmaxA} and $A_{\max}$, respectively) or within each biochemical subtype (Fig. S5).

We found that both V_{pmaxA} and $A_{\max}$ were higher when plants were grown indoors than in the field ($P = 0.005$ and 0.018 for V_{pmaxA} and $A_{\max}$, respectively; Fig. 3E&F), where averaged mean $T_{\max}$ values were 28.2 and 25.2°C, respectively, for indoor and field plants. Specifically, the models estimated that V_{pmaxA} of indoor plants was 35% higher than their outdoor counterparts (55.3 ± 1.7 versus 40.0 ± 2.1 μmol m^{-2} s^{-1}), while $A_{\max}$ of indoor-grown plants was 22% higher than those grown outdoors (33.9 ± 0.9 versus 26.8 ± 1.1 μmol m^{-2} s^{-1}). It is worth noting that C_4 model species (i.e. maize and sorghum) appear to be at the high-end of the V_{pmaxA} and $A_{\max}$ spectrum, particularly for outdoor-grown plants (Fig 3E&F). We thus further examined whether there was an interaction between species group and growth location, and found it to be significant ($P < 0.001$). The mean values of V_{pmaxA} and $A_{\max}$ were significantly higher in outdoor-grown C_4 model species compared to non-model species grown outside ($P < 0.001$; Fig. 4). However, no significant differences were observed between model and non-model species grown indoors. Our results suggest that the lower V_{pmaxA} and $A_{\max}$ values of C_4 non-model species grown outdoors compared to their indoor counterparts could have been attributed to the effect of growth location on photosynthetic capacity.

We also found that V_{pmaxA} and A_{max} decreased significantly with increasing mean T_{max} ($P = 0.001$; Fig. 5A&B), with this pattern being stronger for a subset of data measured at a T_{leaf} between 25 and 30°C to account for variation in T_{leaf} in the analysis (Fig. S6). No effect of growth CO_2 concentrations was found on either V_{pmaxA} or A_{max} (Fig. 5C&D). In contrast to the negative response to mean T_{max}, V_{pmaxA} and A_{max} increased significantly with increasing T_{leaf} ($P < 0.0001$; Fig. 6A&B) and *PPFD* ($P < 0.0001$; Fig. 6C&D). These results highlight the different responses of V_{pmaxA} and A_{max} to short-term changes in T_{leaf} and long-term acclimation to mean T_{max} (see below). Nonetheless, neither the effect of mean T_{max} nor T_{leaf} on V_{pmaxA} or A_{max} was explained by the growth location (Fig. 5A&B; Fig. 6A&B). We further examined whether different C_4 subtypes or growth forms varied in their response to mean T_{max}, T_{leaf} and *PPFD* by considering interaction effects. None of the interaction terms was significant (Table 1), suggesting responses of V_{pmaxA} and A_{max} to growth and measuring temperatures and irradiance are independent of species-specific traits (such as growth form). Overall, the fixed effects considered in our models accounted for 51 and 47% of the variation in V_{pmaxA} and A_{max}, respectively (Table 1).

Interactive effects of T_{leaf} and mean T_{max} on photosynthetic capacity

The different responses of V_{pmaxA} and A_{max} to changes in long-term mean T_{max} and short-term T_{leaf} pointed towards a possible interaction between these two temperature factors (Fig. 5&6). We thus explored the mean $T_{\mathrm{max}} \times T_{\mathrm{leaf}}$ interaction and the result showed that the V_{pmaxA} was not affected by the interaction between growth and measurement temperatures ($P = 0.724$; Table 1), although the interaction term was significant for A_{max} ($P = 0.033$). We further illustrated the complex responses of V_{pmaxA} and A_{max} to mean T_{max} and T_{leaf} using contour plots (Fig. 7). The contour plots show that at any given mean T_{max}, the sensitivity of V_{pmaxA} to changes in T_{leaf} was not influenced by acclimation to different mean T_{max} (Fig. 7A). This pattern also means that V_{pmaxA} measured at the predominant leaf temperatures of warm-grown plants is higher compared to V_{pmaxA} measured at the predominant leaf temperatures of plants grown at lower temperatures. A_{max} also increased with increasing T_{leaf}, but the increase in A_{max} per 1°C increase in T_{leaf} was higher in plants grown in cooler environments (i.e. mean $T_{\mathrm{max}} < 25$°C) compared to warmer environments (Fig. 7B). This suggests that A_{max} was more sensitive to changes in T_{leaf} in plants acclimated to lower mean T_{max}. This pattern highlights that while A_{max} is lower in plants grown and measured at 20°C, compared to those grown and measured at 30°C and 38°C, A_{max} in plants grown and measured at 30°C and 38°C is similar (Fig. 7B).

Impact of C_4 model species on the analysis

Maize, sorghum and *Setaria viridis*, three frequently studied species in C_4 research, dominated our A/C_i dataset (Fig. S1). In fact, data collected from these C_4 model species are widely used to model the response of C_4 non-model species at the ecosystem level [e.g. in the Community Land Model (Lawrence *et al.*, 2019)]. Consequently, we investigated whether V_{pmaxA} and A_{max} of these C_4 model species are representative of the non-model species. We found no significant difference in V_{pmaxA} and A_{max} between the C_4 model and non-model species ($P = 0.230$ and 0.155 for V_{pmaxA} and A_{max}, respectively; Table 1 – species group). However, it is worth noting that the interaction between species group and growth location was significant, due to the lower photosynthetic capacity of non-model species grown outdoors (see above and Fig. 4). Therefore, we suggest that while our results show that C_4 model species have similar photosynthetic capacity compared to non-model species, care must be taken when extending this finding to natural outdoor settings, the conditions of most interest to ecologists and Earth System Model modellers. Lastly, our results indicate that our multivariate model was not biased by the weighting of data from C_4 model species.

Discussion

This study aimed to explore general patterns of C_4 photosynthetic capacity, indicated by V_{pmaxA} and A_{max}, among a wide range of species grown and measured at various conditions. We found that V_{pmaxA} and A_{max} were tightly coupled in a way that reflects the limitation states of C_4 photosynthesis at different C_i and T_{leaf} conditions, supporting Hypothesis 1 (Fig. 2), though this correlation breaks down at higher temperatures. V_{pmaxA} and A_{max} were similar among the three C_4 subtypes and two growth forms, rejecting Hypothesis 2 (Fig. 3A-D), but were influenced by growth and measurement conditions. Indoor plants exhibited higher V_{pmaxA} and A_{max} compared to their outdoor counterparts, supporting Hypothesis 3 (Fig. 3E&F). Both V_{pmaxA} and A_{max} decreased with increasing mean growth T_{max}, supporting Hypothesis 4 (Fig. 5A&B). Both V_{pmaxA} and A_{max} increased with increasing measurement T_{leaf} and *PPFD*, providing partial support for Hypothesis 5 (Fig. 6). Interestingly, the response of A_{max} to T_{leaf} depended on mean T_{max}, indicating that thermal acclimation alters the thermal sensitivity of photosynthetic capacity in C_4 species (Fig. 7). There was no significant effect of growth CO_2 concentration on photosynthetic capacity, leading us to accept Hypothesis 6, though more data are needed at low and high growth CO_2 concentrations to further confirm this result (Fig. 5C&D). Lastly, we explored whether the more commonly measured C_4

model species (maize, sorghum and *Setaria viridis*) were good representatives of a wide range of C_4 plants. We found no evidence of generalised superior photosynthetic capacity in C_4 model species when compared to non-model species (e.g. native C_4 grasses and eudicots as a whole), in opposition to Hypothesis 7 (Table 1), although C_4 model species had higher photosynthetic capacity than non-model species when grown outdoors (Fig. 4). Overall, our analysis highlights that C_4 photosynthesis is strongly affected by growth and measurement conditions but is largely similar across C_4 species from different biochemical subtypes and growth forms. We discuss the potential reasons and consequences of our findings below.

Coupling between V_{pmaxA} and A_{max} reflects photosynthetic limitations

We found a strong positive correlation between estimated V_{pmaxA} and A_{max} in the T_{leaf} range of 25-30°C (Fig. 2B). At T_{leaf} above 30°C, the positive correlation between V_{pmaxA} and A_{max} weakened, with A_{max} showing less pronounced change per unit increase in V_{pmaxA} (Fig. 2C-D). This result agrees with findings derived from flux control analysis (von Caemmerer & Furbank, 2016) and data syntheses (Pignon & Long, 2020), and highlights differences in the temperature-dependent responses of biochemical processes underpinning V_{pmaxA} and A_{max}, such that A_{max} was less temperature sensitive at high T_{leaf} than V_{pmaxA}. The A_{max} in C_4 plants is primarily determined by the maximum carboxylation activity of Rubisco (V_{cmax}) and the rate of RuBP regeneration at high C_{i}, with a reduction in either of these leading to a lower A_{max} (Furbank *et al.*, 1996; von Caemmerer *et al.*, 1997; von Caemmerer & Furbank, 1999). At high T_{leaf}, Rubisco inactivation due to a decrease in Rubisco activase activity (Hendrickson *et al.*, 2008; Salesse-Smith *et al.*, 2018) reduces V_{cmax} and ultimately A_{max}. The RuBP regeneration rate can be limiting when measurement *PPFD* or the capacity of Calvin cycle enzymes, other than Rubisco, limit net CO_2 assimilation rate at high C_{i}, or when the thylakoid membrane is damaged at high temperatures (Peixoto & Sage, 2017). The limitation imposed by RuBP regeneration is expected to be pronounced in C_4 plants, which have lower concentrations of RuBP compared to C_3 plants (Arrivault *et al.*, 2019). However, this limitation is likely not related to the abundance and activity of sedoheptulose-1,7-bisphosphatase (a rate-limiting enzyme in Calvin cycle) (Ermakova *et al.* 2022). An RuBP limitation could further constrain photosynthesis as C_{i} increases, as an increase in C_{i} promotes Rubisco carboxylase activity and leads to more RuBP being consumed. In our dataset, the majority of A/C_{i} measurements were done at $PPFD >$ 1,500 μmol photon m^{-2} s^{-1}, including those measured at $T_{\mathrm{leaf}} > 35$°C (Fig. S7). However, photosynthesis in C_4 plants is usually not light-saturated even at 1,500 μmol photon m^{-2} s^{-1} (Ermakova *et al.*, 2019, 2023).

There is evidence that due to adaption to tropical/subtropical climates where high-light environments are common, C_4 plants evolved a series of photosynthetic traits that allow them to grow under high light (Wasilewska-Dębowska *et al.*, 2022). Adaptation to high light conditions may arguably put C_4 plants at a disadvantage in light conditions that are suboptimal for them but saturating for C_3 plants. These findings highlight the complex interplay between temperature, biochemical limitations, and light availability in regulating C_4 photosynthesis, which in part has become a bottleneck for C_4 photosynthesis modelling at the ecosystem level (Knauer *et al.*, 2023).

Photosynthetic capacity is similar across biochemical types and growth forms

Our results show that variation in C_4 biochemical subtypes and growth forms does not lead to systematic variation in photosynthetic capacity (Fig. 3A-D). In general, popular model species (C_4 NADP-ME type grasses: maize, sorghum and *Setaria viridis*) exhibit similar photosynthetic capacity when compared to non-model C_4 species representing the three C_4 biochemical subtypes (Table 1). However, when growth location is considered, photosynthetic capacity of C_4 model species is higher than that of non-model species when both are grown outdoors (Fig. 4). These results suggest that photosynthetic capacity data collected from model species could overestimate the productivity of non-model species in outdoor conditions. These findings are particularly important for the modelling community, given that the current C_4 vegetation model at the ecosystem level was developed based on parameters measured in maize grown in controlled environments (Collatz *et al.*, 1992; Lawrence *et al.*, 2019), and likely overestimates the productivity of C_4 native and eudicots grown in the field. The lack of a significant effect of C_4 subtypes on photosynthetic capacity further emphasises the biochemical flexibility in the C_4 pathway. There is growing molecular, biochemical and physiological evidence suggesting that the three classical subtypes, originally defined based on early ^{14}C-labelling studies (Hatch & Slack, 1970; Hatch, 1971), can be biochemically flexible (Furbank, 2011; Bräutigam *et al.*, 2014; Wang *et al.*, 2014; Sales *et al.*, 2021), which in turn diminishes any potential differences in photosynthetic capacity among the subtypes. This biochemical flexibility may be regulated by developmental and environmental variation, further highlighting the role of environmental effects on C_4 photosynthesis (see below).

Growth location affects photosynthetic capacity

Our results showed that growth and measurement conditions are the major factors affecting photosynthetic capacity in C_4 plants. Indoor plants exhibit consistently higher V_{pmaxA} and A_{max} than their outdoor counterparts (Fig. 3E&F), despite indoor plants being grown in warmer environments which might suppress photosynthetic capacity (Fig. S4A). Plants grown in indoor, controlled environments are usually well-watered and fertilised, and are not challenged with pests and extreme conditions (e.g. heat waves or frost stress) (Poorter *et al.*, 2016). The lower photosynthetic capacity in outdoor non-model species is likely due to the more stressful conditions they experience, which are primarily characterised by lower water and nutrient availability than indoor-grown plants. For example, long-term drought (i.e. >100 days) could cause significant reductions in stomatal conductance, net photosynthetic rate and V_{pmaxA}, with such effects being exacerbated in N-limited C_4 plants (Markelz *et al.*, 2011). Interestingly, the impact of drought on photosynthetic capacity (i.e. A_{max}) was not seen in two well-fertilised C_4 grasses, *Dactyloctenium aegyptium* and *Schoenefeldia gracilis* (Maroco *et al.*, 2000), suggesting changes in photosynthetic capacity may be associated with interactive effects of drought and N limitation on plants. In contrast, C_4 model species—particularly maize and sorghum—have been selectively bred for improved drought tolerance (Lopes *et al.*, 2011) and are typically well-watered and well-fertilised in crop fields due to their high agricultural value. These effects may have contributed to higher photosynthetic capacity in C_4 model species grown outdoors (Fig. 4). Further research is needed to dissect the mechanism underpinning the combined effects of drought and N limitation on photosynthesis and to identify why outdoor growth conditions affect non-model species more than model C_4 species.

Temperature significantly influences photosynthetic capacity

We observed that both V_{pmaxA} and A_{max} decreased with increasing mean T_{max} (Fig. 5A&B). This finding is supported by previous work (Berry & Bjorkman, 1980) and aligns with our knowledge of thermal acclimation (Way & Yamori, 2014). Plants grown in warmer conditions often reduce photosynthetic capacity (i.e. V_{pmaxA} and A_{max}), while maintaining comparable (or even higher) A at their growth temperatures compared to control plants. This decrease in photosynthetic capacity is likely due to reduced photosynthetic enzyme concentrations. Warmer temperatures allow plants to achieve the same rate of photosynthesis with lower enzyme concentrations because higher temperatures enhance enzyme activity (Yamori *et al.*, 2014; Way & Yamori, 2014). Evidence supports this idea in C_4 plants: Dwyer *et al.* (2007) compared C_4 *Panicum coloratum*, *Cenchrus ciliaris* and *Flaveria bidentis* grown at moderate and high temperatures and found that warm-grown plants had reduced photosynthetic capacity (i.e. A_{max}), underpinned by lower concentrations of Rubisco and chloroplastic electron transport chain proteins. However, the authors did not find a significant effect of growth temperature on the activity or concentration of PEPc (measured at the respective growth temperatures), suggesting that PEPc may have high thermal stability (Chen *et al.*, 1994; Chinthapalli *et al.*, 2002; Boyd *et al.*, 2015). Thus, it is possible that the decrease in V_{pmaxA} with increasing mean T_{max} observed in our study may be reflective of changes in PEP regeneration via PPDK rather than PEPc capacity *per se*. In *Miscanthus* × *giganteus*, the activity and capacity of PPDK per unit leaf area increases in plants grown at chilling temperature, compared to their warm-grown controls (Wang *et al.*, 2008). Furthermore, whether A/C_{i} measurements are taken at saturated *PPFD* may also affect PEP regeneration, which requires two photosynthetically-generated ATP per PEP converted (Hatch, 1987). Although some of the measurements in our dataset were made at *PPFD* $< 1000\ \mu\mathrm{mol\ m^{-2}\ s^{-1}}$, we found no significant effect of lower measurement *PPFD* on the responses of V_{pmaxA} and A_{max} to intrinsic or extrinsic factors (Table 1; Table S1). Further research is needed to explore how PEPc and PPDK capacities are coordinated under thermal acclimation.

Our results highlight that both V_{pmaxA} and A_{max} increase with measurement T_{leaf} (Fig. 6A&B), which is indicative of enhanced enzymatic activities at higher measurement temperatures. According to an *in vitro* study in *Setaria viridis*, the capacities of major C_4 photosynthetic enzymes generally increase with rising T_{leaf} due to a corresponding rise in enzyme activities (Boyd *et al.*, 2015). The carboxylation activities of Rubisco and PEPc increase exponentially between 10°C and 40–45°C, before declining (Chen *et al.*, 1994; Chinthapalli *et al.*, 2002; Boyd *et al.*, 2015). However, the extent to which this temperature response of enzymes holds true *in vivo* remains uncertain and needs to be confirmed with high-resolution photosynthesis-temperature response curves across a diverse range of C_4 species.

Finally, our analysis highlights that the response of A_{max} to T_{leaf} is influenced by mean T_{max}, whereas that of V_{pmaxA} is not (Table 1; Fig. 7). We found that A_{max} increases to a greater extent with increasing T_{leaf} in cool-grown plants compared to plants grown in warmer conditions, suggesting that A_{max} of cool-grown plants is more sensitive to changes in T_{leaf} (Fig. 7B). This finding has implications for the photosynthetic performance of C_4 plants under future climates. In a high CO_2 world, C_4 plants will be able to achieve photosynthetic performance closer to their maximum potential (i.e. A_{max}), as higher atmospheric [CO_2] increases C_{i} and moves plants away from potential V_{pmaxA} limitations of photosynthesis. Our data suggest that A_{max} of C_4 plants grown under future, hotter climates will be less affected by daily temperature fluctuations compared to plants grown under the current climate (i.e. A_{max} will be more stable; see circles in Fig. 7). This reduced thermal sensitivity of A_{max} at higher temperatures may help buffer photosynthesis in future climates, where heat waves are predicted to occur more frequently and intensely (Brown, 2020). However, this response could also limit the ability of warm-grown C_4 plants to achieve high A_{max} at the high T_{leaf} conditions they will experience (Fig. 7), which may suppress CO_2 uptake in future climate conditions. As we saw no effect of elevated growth CO_2 concentrations on either V_{pmaxA} or $A_{\max}$ (Fig. 5C&D), in line with field studies of C_4 species (Leakey *et al.*, 2006; Leakey, 2009; Markelz *et al.*, 2011), these temperature effects are likely to be stronger controls on C_4 photosynthetic capacity in future climates than predicted increases in CO_2 levels. However, further research is needed to fully understand how climate change affects the photosynthetic physiology of C_4 plants.

Future perspectives

Looking forward, our analyses highlight areas where more studies are warranted. For example, the physiology of C_4 eudicots and sedges is underrepresented in our dataset, although eudicots and sedges comprise 38% of C_4 plants (Sage, 2017) and thrive in extreme environments [e.g. *Haloxylon*, a C_4 desert shrub (Feng *et al.*, 2023)]. Understanding how C_4 photosynthesis responds to these extreme environments could provide insights into improving how other plants (e.g. C_3 crops) cope with extreme environments. Furthermore, our results show that $A_{\max}$ responds differently to growth and measurement temperatures than does V_{pmaxA}. We explored potential biochemical limitations that underpin $A_{\max}$ and V_{pmaxA} separately, in addition to the response of these limitations to changes in temperature. However, it is unclear to what extent the individual biochemical limitations may interact and affect overall photosynthetic capacity. If one assumes that PEP regeneration is not limited, V_{pmaxA} is largely determined by the property of PEPc (e.g. activation state and activity of the enzyme) and its temperature sensitivity likely reflects the temperature sensitivity of PEPc. In contrast, $A_{\max}$ is determined by a variety of biochemical processes (e.g. Rubisco carboxylation, rates of electron transport). Therefore, understanding how these processes interact in response to changing temperatures is crucial for fully grasping the overall response of $A_{\max}$.

Conclusion

C_4 plants play a crucial role in carbon exchange and food security on a global scale. There has been a growing number of studies dissecting the mechanism of C_4 photosynthesis in specific contexts, yet how C_4 photosynthetic capacity responds to differences in biochemical subtypes, plant functional types, and growth and measurement conditions among a wide range of species remains unclear. Our study uncovers broad patterns of photosynthetic capacity from 74 C_4 species and highlights that environmental conditions play a dominant role in determining C_4 photosynthetic capacity. Importantly, we demonstrate that while the current simplified parameterisation of C_4 NADP-ME-type photosynthesis in leaf- and ecosystem-level models likely represents species of all three biochemical types, it overestimates the photosynthetic capacity of C_4 native species in the field conditions. Future research should aim to refine current parameter values by incorporating detailed equations that capture the effects of abiotic factors, such as water and nutrient availability, on photosynthetic capacity (Smith *et al.*, 2019), while also examining their link to the leaf economics spectrum (Monson *et al.*, 2025). Additionally, we compile a C_4 A/C_i database for community use, addressing the shortage of accessible raw data for C_4 gas exchange. For example, the TRY leaf-trait database (http://www.try-db.org), one of the most comprehensive databases of plant physiological trait data in the world, contains leaf photosynthetic point measurements for only 591 C_4 species, out of 69,000 terrestrial species measured, and no C_4 photosynthetic response curves (Kattge *et al.*, 2011, 2020). Our database opens new avenues for future studies involving big data analysis for C_4 plants, such as simulation modelling.

Acknowledgements

This work was conducted as part of the C_4 Photosynthesis Working Group supported by the John Wesley Powell Center for Analysis and Synthesis, funded by the US Geological Survey Award Number 20-07-0232. Additional support for D.A.W. came from The Australian National University Futures Scheme, and for Y.F. from an Australian Research Council Discovery Project (DP230103122). D.W.A.N. was supported by an ARC Future Fellowship (FT220100276). A.D.B.L. was supported by the DOE Center for Advanced Bioenergy and Bioproducts Innovation (U.S. Department of Energy, Office of Science, Biological and Environmental Research Program under Award Number DE-SC0018420). F.A.B. was supported by the Natural Environment Research Council (NE/W00674X/1). K.P. was supported by U.S. National Science Foundation grants (IOS-2312181, IOS-2406533, IOS-1546838, MCB-1617020; DBI-2213983 and OISE-2434687), U.S. Department of Energy, Office of Science, Office of Biological and Environmental Research, Genomic Science Program grants (DE-SC0018277, DE-SC0020366, DE-SC0023160, and DE-SC0021286, and DE-SC0008769), and Carnegie Venture Grant (10908). M.L. is supported by an Australian Research Council Discovery Project (DP130102243). Any use of trade, firm, or product names is for descriptive purposes only and does not imply endorsement by the U.S. Government.

Conflict of interest

None declared.

Author contribution

D.A.W. conceived the concept for the paper within the discussions provided by the US Geological Survey Powell Center C_4 Working Group. Y.F. complied the dataset, coded the scripts and ran the analyses with help from D.W.A.N. and B.E.M. N.G.S., E.A.A., F.A.B., F.R.D., M.E., P.F., R.T.F., S.H.G., O.G., L.G., V.J., A.D.B.L., S.L., M.L., V.S.P., M.M.P., B.V.S., S.v.C., R.W. and D.A.W. provided data to this study. Y.F. and D.A.W. wrote the first draft, and all authors contributed substantially to improving the draft.

Data availability

Upon publication, all data will be available as a Supplementary Dataset and downloadable from GitHub.

Supplementary material

Dataset S1 – C_4 A/C_i data collated for this study.

Dataset S2 – Estimated apparent V_pmaxA and A_max used in the analysis.

Table S1 – Results of multivariate linear mixed-effects models for data with $PPFD > 1000$ μmol photon $\mathrm{m^{-2}\ s^{-1}}$.

Figure S1 – Species distribution within the categories of growth forms and growth locations.

Figure S2 – Correlation of mean T_max and T_min.

Figure S3 – Data distribution of V_pmaxA and A_max in categories of C_4 subtypes and growth forms over T_leaf, mean T_max and *PPFD*.

Figure S4 – Histograms describing the data distribution across the spectrum of mean T_max and T_leaf for growth location, growth form and important species group.

Figure S5 – V_pmaxA and A_max plotted by C_4 biochemical subtypes, with symbols highlighting the effect of phylogeny.

Figure S6 – Relationships between V_pmaxA and A_max with mean T_max for measurements done at T_leaf between 25 and 30°C.

Figure S7 – Correlation of mean T_max and T_min for data with $PPFD > 1{,}500$ μmol photon $\mathrm{m^{-2}\ s^{-1}}$.

Reference

Anderson LJ, Maherali H, Johnson HB, Polley HW, Jackson RB. **2001**. Gas exchange and photosynthetic acclimation over subambient to elevated CO_2 in a C_3–C_4 grassland. *Global Change Biology* **7**: 693–707.

Arena C, Vitale L, De Santo AV. **2011**. Influence of irradiance on photosynthesis and PSII photochemical efficiency in maize during short-term exposure at high CO_2 concentration. *Photosynthetica* **49**: 267–274.

Arrivault S, Alexandre Moraes T, Obata T, Medeiros DB, Fernie AR, Boulouis A, Ludwig M, Lunn JE, Borghi GL, Schlereth A, *et al.* 2019. Metabolite profiles reveal interspecific variation in operation of the Calvin–Benson cycle in both C_4 and C_3 plants. *Journal of Experimental Botany* **70**: 1843–1858.

Atkin OK, Tjoelker MG. **2003**. Thermal acclimation and the dynamic response of plant respiration to temperature. *Trends in Plant Science* **8**: 343–351.

Bauwe H. **1986**. An efficient method for the determination of K_m values for HCO_3^- of phosphoenolpyruvate carboxylase. *Planta* **169**: 356–360.

Berry J, Bjorkman O. **1980**. Photosynthetic Response and Adaptation to Temperature in Higher Plants. *Annual Review of Plant Biology* **31**: 491–543.

Bissinger K, Khoshravesh R, Kotrade JP, Oakley J, Sage TL, Sage RF, Hartmann HEK, Kadereit G. **2014**. *Gisekia* (Gisekiaceae): Phylogenetic relationships, biogeography, and ecophysiology of a poorly known C_4 lineage in the Caryophyllales. *American Journal of Botany* **101**: 499–509.

Bloom AJ, Asensio JSR, Randall L, Rachmilevitch S, Cousins AB, Carlisle EA. **2012**. CO_2 enrichment inhibits shoot nitrate assimilation in C_3 but not C_4 plants and slows growth under nitrate in C_3 plants. *Ecology* **93**: 355–367.

Boyd RA, Gandin A, Cousins AB. **2015**. Temperature Responses of C_4 Photosynthesis: Biochemical Analysis of Rubisco, Phospho*enol*pyruvate Carboxylase, and Carbonic Anhydrase in *Setaria viridis*. *Plant Physiology* **169**: 1850–1861.

Bräutigam A, Schliesky S, Külahoglu C, Osborne CP, Weber APM. **2014**. Towards an integrative model of C_4 photosynthetic subtypes: insights from comparative transcriptome analysis of NAD-ME, NADP-ME, and PEP-CK C_4 species. *Journal of Experimental Botany* **65**: 3579–3593.

Brown SJ. **2020**. Future changes in heatwave severity, duration and frequency due to climate change for the most populous cities. *Weather and Climate Extremes* **30**: 100278.

von Caemmerer S. **2000**. Modeling C_4 photosynthesis. In: Biochemical models of leaf photosynthesis. Collingwood, Australia: CSIRO Publishing, 91–122.

von Caemmerer S. **2021**. Updating the steady-state model of C_4 photosynthesis. *Journal of Experimental Botany* **72**: 6003–6017.

von Caemmerer S, Evans JR, Hudson GS, Andrews TJ. **1994**. The kinetics of ribulose-1,5-bisphosphate carboxylase/oxygenase in vivo inferred from measurements of photosynthesis in leaves of transgenic tobacco. *Planta* **195**: 88–97.

von Caemmerer S, Furbank RT. **1999**. Modeling C_4 Photosynthesis. In: Sage RF, Monson RK, eds. C_4 Plant Biology. San Diego: Academic Press, 173–211.

von Caemmerer S, Furbank RT. **2016**. Strategies for improving C_4 photosynthesis. *Current Opinion in Plant Biology* **31**: 125–134.

von Caemmerer S, Millgate A, Farquhar GD, Furbank RT. **1997**. Reduction of Ribulose-1,5-Bisphosphate Carboxylase/Oxygenase by Antisense RNA in the C_4 Plant *Flaveria bidentis* Leads to Reduced Assimilation Rates and Increased Carbon Isotope Discrimination. *Plant Physiology* **113**: 469–477.

Carmo-Silva AE, Powers SJ, Keys AJ, Arrabaça MC, Parry MAJ. **2008**. Photorespiration in C_4 grasses remains slow under drought conditions. *Plant, Cell & Environment* **31**: 925–940.

Cavaco AM, Da Silva AB, Arrabaça MC. **2003**. Effects of long-term chilling on growth and photosynthesis of the C_4 gramineae *Paspalum dilatatum*. *Physiologia Plantarum* **119**: 87–96.

Chen D-X, Coughenour MB, Knapp AK, Owensby CE. **1994**. Mathematical simulation of C_4 grass photosynthesis in ambient and elevated CO_2. *Ecological Modelling* **73**: 63–80.

Chen J-W, Yang Z-Q, Zhou P, Hai M-R, Tang T-X, Liang Y-L, An T-X. **2013**. Biomass accumulation and partitioning, photosynthesis, and photosynthetic induction in field-grown maize (*Zea mays* L.) under low- and high-nitrogen conditions. *Acta Physiologiae Plantarum* **35**: 95–105.

Chinthapalli B, Raghavendra AS, Rishi AS, Arun G. **2002**. Phosphonelopyruvate carboxylase from C_4 plants: properties and regulation. *Reviews in Plant Biochemistry and Biotechnology* **1**: 143–159.

Collatz GJ, Ribas-Carbo M, Berry JA. **1992**. Coupled Photosynthesis-Stomatal Conductance Model for Leaves of C_4 Plants. *Functional Plant Biology* **19**: 519–538.

Cousins AB, Bloom AJ. **2003**. Influence of elevated CO_2 and nitrogen nutrition on photosynthesis and nitrate photo-assimilation in maize (*Zea mays* L.). *Plant, Cell & Environment* **26**: 1525–1530.

Cowling SA, Jones CD, Cox PM. **2007**. Consequences of the evolution of C_4 photosynthesis for surface energy and water exchange. *Journal of Geophysical Research: Biogeosciences* **112**.

Cunniff J, Jones G, Charles M, Osborne CP. **2017**. Yield responses of wild C_3 and C_4 crop progenitors to subambient CO_2: a test for the role of CO_2 limitation in the origin of agriculture. *Global Change Biology* **23**: 380–393.

Cunniff J, Osborne CP, Ripley BS, Charles M, Jones G. **2008**. Response of wild C_4 crop progenitors to subambient CO_2 highlights a possible role in the origin of agriculture. *Global Change Biology* **14**: 576–587.

Danila FR, Thakur V, Chatterjee J, Bala S, Coe RA, Acebron K, Furbank RT, von Caemmerer S, Quick WP. **2021**. Bundle sheath suberisation is required for C_4 photosynthesis in a *Setaria viridis* mutant. *Communications Biology* **4**: 254.

DiMario RJ, Cousins AB. **2019**. A single serine to alanine substitution decreases bicarbonate affinity of phosphoenolpyruvate carboxylase in C_4 *Flaveria trinervia*. *Journal of Experimental Botany* **70**: 995–1004.

Ding R, Xie J, Mayfield-Jones D, Zhang Y, Kang S, Leakey ADB. **2022**. Plasticity in stomatal behaviour across a gradient of water supply is consistent among field-grown maize inbred lines with varying stomatal patterning. *Plant, Cell & Environment* **45**: 2324–2336.

Dwyer SA, Ghannoum O, Nicotra A, von Caemmerer S. **2007**. High temperature acclimation of C_4 photosynthesis is linked to changes in photosynthetic biochemistry. *Plant, Cell & Environment* **30**: 53–66.

Ermakova M, Lopez-Calcagno PE, Furbank RT, Raines CA, von Caemmerer S. **2022**. Increased sedoheptulose-1,7-bisphosphatase content in Setaria viridis does not affect C_4 photosynthesis. *Plant Physiology* **191**: 885–893.

Ermakova M, Lopez-Calcagno PE, Raines CA, Furbank RT, von Caemmerer S. **2019**. Overexpression of the Rieske FeS protein of the Cytochrome b6f complex increases C_4 photosynthesis in *Setaria viridis*. *Communications Biology* **2**: 1–12.

Ermakova M, Woodford R, Fitzpatrick D, Nix SJ, Zwahlen SM, Farquhar GD, von Caemmerer S, Furbank RT. **2024**. Chloroplast NADH dehydrogenase-like complex-mediated cyclic electron flow is the main electron transport route in C_4 bundle sheath cells. *New Phytologist* **243**: 2187–2200.

Ermakova M, Woodford R, Taylor Z, Furbank RT, Belide S, von Caemmerer S. **2023**. Faster induction of photosynthesis increases biomass and grain yield in glasshouse-grown transgenic *Sorghum bicolor* overexpressing Rieske FeS. *Plant Biotechnology Journal* **21**: 1206–1216.

Evans JR. **1989**. Photosynthesis and nitrogen relationships in leaves of C_3 plants. *Oecologia* **78**: 9–19.

Evans JR, von Caemmerer S. **1996**. Carbon dioxide diffusion inside leaves. *Plant Physiology* **110**: 339–346.

Fan Y, Asao S, Furbank RT, von Caemmerer S, Day DA, Tcherkez G, Sage TL, Sage RF, Atkin OK. **2022**. The crucial roles of mitochondria in supporting C_4 photosynthesis. *New Phytologist* **233**: 1083–1096.

Fay PA, Jin VL, Way DA, Potter KN, Gill RA, Jackson RB, Wayne Polley H. **2012**. Soil-mediated effects of subambient to increased carbon dioxide on grassland productivity. *Nature Climate Change* **2**: 742–746.

Feng XP, Chen Y, Qi YH, Yu CL, Zheng B-S, Brancourt-Hulmel M, Jiang D-A. **2012**. Nitrogen enhanced photosynthesis of Miscanthus by increasing stomatal conductance and phosphoenolpyruvate carboxylase concentration. *Photosynthetica* **50**: 577–586.

Feng X, Liu R, Li C, Zhang H, Slot M. **2023**. Contrasting responses of two C_4 desert shrubs to drought but consistent decoupling of photosynthesis and stomatal conductance at high temperature. *Environmental and Experimental Botany* **209**: 105295.

Friedlingstein P, O'Sullivan M, Jones MW, Andrew RM, Hauck J, Landschützer P, Le Quéré C, Li H, Luijkx IT, Olsen A, *et al.* **2025**. Global Carbon Budget 2024. *Earth System Science Data* **17**: 965–1039.

Friesen PC, Peixoto MM, Busch FA, Johnson DC, Sage RF. **2014**. Chilling and frost tolerance in *Miscanthus* and *Saccharum* genotypes bred for cool temperate climates. *Journal of Experimental Botany* **65**: 3749–3758.

Furbank RT. **2011**. Evolution of the C_4 photosynthetic mechanism: are there really three C_4 acid decarboxylation types? *Journal of Experimental Botany* **62**: 3103–3108.

Furbank RT, Chitty JA, von Caemmerer S, Jenkins CLD. **1996**. Antisense RNA Inhibition of RbcS Gene Expression Reduces Rubisco Level and Photosynthesis in the C_4 Plant *Flaveria bidentis*. *Plant Physiology* **111**: 725–734.

Gan SH, Sage RF. **2024**. Stomatal response to VPD in C_4 plants with different biochemical sub-pathways. *Plant, Cell & Environment* **47**: 3466–3477.

Ge ZM, Zhang LQ, Yuan L, Zhang C. **2014**. Effects of salinity on temperature-dependent photosynthetic parameters of a native C_3 and a non-native C_4 marsh grass in the Yangtze Estuary, China. *Photosynthetica* **52**: 484–492.

Ghannoum O, Caemmerer SV, Ziska LH, Conroy JP. **2000**. The growth response of C_4 plants to rising atmospheric CO_2 partial pressure: a reassessment. *Plant, Cell & Environment* **23**: 931–942.

Ghannoum O, Evans JR, von Caemmerer S. **2011**. Nitrogen and water use efficiency of C_4 plants. In: Raghavendra AS, Sage RF, eds. C_4 photosynthesis and related CO_2 concentrating mechanisms. Dordrecht: Springer, 129–146.

Głowacka K, Jørgensen U, Kjeldsen JB, Kørup K, Spitz I, Sacks EJ, Long SP. **2015**. Can the exceptional chilling tolerance of C_4 photosynthesis found in *Miscanthus* × *giganteus* be exceeded? Screening of a novel *Miscanthus* Japanese germplasm collection. *Annals of Botany* **115**: 981–990.

Griffith DM, Osborne CP, Edwards EJ, Bachle S, Beerling DJ, Bond WJ, Gallaher TJ, Helliker BR, Lehmann CER, Leatherman L, *et al.* 2020. Lineage-based functional types: characterising functional diversity to enhance the representation of ecological behaviour in Land Surface Models. *New Phytologist* **228**: 15–23.

Hatch MD. **1971**. The C_4-pathway of photosynthesis: evidence for an intermediate pool of carbon dioxide and the identity of the donor C_4-dicarboxylic acid. *Biochemical Journal* **125**: 425–432.

Hatch MD. **1987**. C_4 photosynthesis: a unique elend of modified biochemistry, anatomy and ultrastructure. *Biochimica et Biophysica Acta* **895**: 81–106.

Hatch MD, Slack CR. **1970**. Photosynthetic CO_2-fixation pathways. *Annual Review of Plant Physiology* **21**: 141–162.

Heckman RW, Pereira CG, Aspinwall MJ, Juenger TE. **2024**. Physiological responses of C_4 perennial bioenergy grasses to climate change: causes, consequences, and constraints. *Annual Review of Plant Biology* **75**: 737–769.

Hendrickson L, Sharwood R, Ludwig M, Whitney SM, Badger MR, von Caemmerer S. **2008**. The effects of Rubisco activase on C_4 photosynthesis and metabolism at high temperature. *Journal of Experimental Botany* **59**: 1789–1798.

Horst RJ, Engelsdorf T, Sonnewald U, Voll LM. **2008**. Infection of maize leaves with *Ustilago maydis* prevents establishment of C_4 photosynthesis. *Journal of Plant Physiology* **165**: 19–28.

Huntingford C, Zelazowski P, Galbraith D, Mercado LM, Sitch S, Fisher R, Lomas M, Walker AP, Jones CD, Booth BB. **2013**. Simulated resilience of tropical rainforests to CO_2-induced climate change. *Nature Geoscience* **6**: 268.

Kakani VG, Boote KJ, Reddy KR, Lang DJ. **2008a**. Response of bahiagrass carbon assimilation and photosystem activity to below optimum temperatures. *Functional Plant Biology* **35**: 1243.

Kakani VG, Surabhi GK, Reddy KR. **2008b**. Photosynthesis and fluorescence responses of C_4 plant *Andropogon gerardii* acclimated to temperature and carbon dioxide. *Photosynthetica* **46**: 420–430.

Kattge J, Bönisch G, Díaz S, Lavorel S, Prentice IC, Leadley P, Tautenhahn S, Werner GDA, Aakala T, Abedi M, *et al.* 2020. TRY plant trait database – enhanced coverage and open access. *Global Change Biology* **26**: 119–188.

Kattge J, Díaz S, Lavorel S, Prentice IC, Leadley P, Bönisch G, Garnier E, Westoby M, Reich PB, Wright IJ, *et al.* 2011. TRY – a global database of plant traits. *Global Change Biology* **17**: 2905–2935.

Khoshravesh R, Stata M, Busch FA, Saladié M, Castelli JM, Dakin N, Hattersley PW, Macfarlane TD, Sage RF, Ludwig M, *et al.* 2020. The evolutionary origin of C_4 photosynthesis in the grass subtribe Neurachninae. *Plant Physiology* **182**: 566–583.

Kim S-H, Sicher RC, Bae H, Gitz DC, Baker JT, Timlin DJ, Reddy VR. **2006**. Canopy photosynthesis, evapotranspiration, leaf nitrogen, and transcription profiles of maize in response to CO_2 enrichment. *Global Change Biology* **12**: 588–600.

Knauer J, Cuntz M, Smith B, Canadell JG, Medlyn BE, Bennett AC, Caldararu S, Haverd V. **2023**. Higher global gross primary productivity under future climate with more advanced representations of photosynthesis. *Science Advances* **9**: eadh9444.

Kubien DS, Sage RF. **2004**. Low-temperature photosynthetic performance of a C_4 grass and a co-occurring C_3 grass native to high latitudes. *Plant, Cell & Environment* **27**: 907–916.

Laisk A, Edwards GE. **1997**. CO_2 and Temperature-dependent Induction in C_4 Photosynthesis: an Approach to the Hierarchy of Rate-limiting Processes. *Functional Plant Biology* **24**: 505–516.

Lawrence DM, Fisher RA, Koven CD, Oleson KW, Swenson SC, Bonan G, Collier N, Ghimire B, van Kampenhout L, Kennedy D, *et al.* 2019. The Community Land Model Version 5: Description of New Features, Benchmarking, and Impact of Forcing Uncertainty. *Journal of Advances in Modeling Earth Systems* **11**: 4245–4287.

Leakey ADB. **2009**. Rising atmospheric carbon dioxide concentration and the future of C_4 crops for food and fuel. *Proceedings of the Royal Society B: Biological Sciences* **276**: 2333–2343.

Leakey ADB, Ferguson JN, Pignon CP, Wu A, Jin Z, Hammer GL, Lobell DB. **2019**. Water Use Efficiency as a Constraint and Target for Improving the Resilience and Productivity of C3 and C4 Crops. *Annual Review of Plant Biology* **70**: 781–808.

Leakey ADB, Uribelarrea M, Ainsworth EA, Naidu SL, Rogers A, Ort DR, Long SP. **2006**. Photosynthesis, productivity, and yield of maize are not affected by open-air elevation of CO_2 concentration in the absence of drought. *Plant Physiology* **140**: 779–790.

Leegood RC. **2002**. C_4 photosynthesis: principles of CO_2 concentration and prospects for its introduction into C_3 plants. *Journal of Experimental Botany* **53**: 581–590.

Li S, Courbet G, Ourry A, Ainsworth EA. **2019**. Elevated ozone concentration reduces photosynthetic carbon gain but does not alter leaf structural traits, nutrient composition or biomass in switchgrass. *Plants* **8**: 85.

Li S, Moller CA, Mitchell NG, Lee D, Ainsworth EA. **2021**. Bioenergy sorghum maintains photosynthetic capacity in elevated ozone concentrations. *Plant, Cell & Environment* **44**: 729–746.

Li S, Moller CA, Mitchell NG, Lee D, Sacks EJ, Ainsworth EA. **2022**. Testing unified theories for ozone response in C_4 species. *Global Change Biology* **28**: 3379–3393.

Liu X, Qiao Y, Zhou W, Dong W, Gu L. **2023**. Determinants of photochemical characteristics of the photosynthetic electron transport chain of maize. *Frontiers in Plant Science* **14**: 1279963.

Liu H, Taylor SH, Xu Q, Lin Y, Hou H, Wu G, Ye Q. **2019**. Life history is a key factor explaining functional trait diversity among subtropical grasses, and its influence differs between C_3 and C_4 species. *Journal of Experimental Botany* **70**: 1567–1580.

Long SP, Woolhouse HW. **1978**. The Responses of Net Photosynthesis to Vapour Pressure Deficit and CO_2 Concentration in *Spartina townsendii* (sensu lato), a C_4 Species from a Cool Temperate Climate. *Journal of Experimental Botany* **29**: 567–577.

Lopes MS, Araus JL, van Heerden PDR, Foyer CH. **2011**. Enhancing drought tolerance in C_4 crops. *Journal of Experimental Botany* **62**: 3135–3153.

Luo X, Zhou H, Satriawan TW, Tian J, Zhao R, Keenan TF, Griffith DM, Sitch S, Smith NG, Still CJ. **2024**. Mapping the global distribution of C_4 vegetation using observations and optimality theory. *Nature Communications* **15**: 1219.

Mantlana KB, Arneth A, Veenendaal EM, Wohland P, Wolski P, Kolle O, Wagner M, Lloyd J. **2008**. Photosynthetic properties of C_4 plants growing in an African savanna/wetland mosaic. *Journal of Experimental Botany* **59**: 3941–3952.

Markelz RJC, Strellner RS, Leakey ADB. **2011**. Impairment of C_4 photosynthesis by drought is exacerbated by limiting nitrogen and ameliorated by elevated [CO_2] in maize. *Journal of Experimental Botany* **62**: 3235–3246.

Maroco JP, Pereira JS, Manuela Chaves M. **2000**. Growth, photosynthesis and water-use efficiency of two C_4 Sahelian grasses subjected to water deficits. *Journal of Arid Environments* **45**: 119–137.

Monson RK, Li S, Ainsworth EA, Fan Y, Hodge JG, Knapp AK, Leakey ADB, Lombardozzi D, Reed SC, Sage RF, *et al.* **2025**. C_4 photosynthesis, trait spectra, and the fast-efficient phenotype. *New Phytologist* **246**: 879–893.

Naidu SL, Moose SP, AL-Shoaibi AK, Raines CA, Long SP. **2003**. Cold tolerance of C_4 photosynthesis in *Miscanthus* × *giganteus*: adaptation in amounts and sequence of C_4 photosynthetic enzymes. *Plant Physiology* **132**: 1688–1697.

Nakagawa S, Lagisz M, O'Dea RE, Pottier P, Rutkowska J, Senior AM, Yang Y, Noble DWA. **2023**. orchaRd 2.0: An R package for visualising meta-analyses with orchard plots. *Methods in Ecology and Evolution* **14**: 2003–2010.

Nakagawa S, Lagisz M, O'Dea RE, Rutkowska J, Yang Y, Noble DWA, Senior AM. **2021**. The orchard plot: Cultivating a forest plot for use in ecology, evolution, and beyond. *Research Synthesis Methods* **12**: 4–12.

Nakagawa S, Santos ESA. **2012**. Methodological issues and advances in biological meta-analysis. *Evolutionary Ecology* **26**: 1253–1274.

Nippert JB, Fay PA, Knapp AK. **2007**. Photosynthetic traits in C_3 and C_4 grassland species in mesocosm and field environments. *Environmental and Experimental Botany* **60**: 412–420.

Noble DWA, Lagisz M, O'dea RE, Nakagawa S. **2017**. Nonindependence and sensitivity analyses in ecological and evolutionary meta-analyses. *Molecular Ecology* **26**: 2410–2425.

Noble DWA, Pottier P, Lagisz M, Burke S, Drobniak SM, O'Dea RE, Nakagawa S. **2022**. Meta-analytic approaches and effect sizes to account for 'nuisance heterogeneity' in comparative physiology. *Journal of Experimental Biology* **225**: jeb243225.

Oakley JC, Sultmanis S, Stinson CR, Sage TL, Sage RF. **2014**. Comparative studies of C_3 and C_4 *Atriplex* hybrids in the genomics era: physiological assessments. *Journal of Experimental Botany* **65**: 3637–3647.

Osborne CP, Wythe EJ, Ibrahim DG, Gilbert ME, Ripley BS. **2008**. Low temperature effects on leaf physiology and survivorship in the C_3 and C_4 subspecies of *Alloteropsis semialata*. *Journal of Experimental Botany* **59**: 1743–1754.

Pathare VS, Koteyeva N, Cousins AB. **2020**. Increased adaxial stomatal density is associated with greater mesophyll surface area exposed to intercellular air spaces and mesophyll conductance in diverse C_4 grasses. *New Phytologist* **225**: 169–182.

Pearcy RW. **1977**. Acclimation of photosynthetic and respiratory carbon dioxide exchange to growth temperature in *Atriplex lentiformis* (Torr.) Wats. *Plant Physiology* **59**: 795–799.

Peixoto M de M, Sage RF. **2017**. Comparative photosynthetic responses in upland and lowland sugarcane cultivars grown in cool and warm conditions. *Brazilian Journal of Botany* **40**: 829–839.

Peixoto MM, Sage TL, Busch FA, Pacheco HDN, Moraes MG, Portes TA, Almeida RA, Graciano-Ribeiro D, Sage RF. **2021**. Elevated efficiency of C_3 photosynthesis in bamboo grasses: A possible consequence of enhanced refixation of photorespired CO_2. *GCB Bioenergy* **13**: 941–954.

Pengelly JJL, Sirault XRR, Tazoe Y, Evans JR, Furbank RT, von Caemmerer S. **2010**. Growth of the C_4 dicot *Flaveria bidentis*: photosynthetic acclimation to low light through shifts in leaf anatomy and biochemistry. *Journal of Experimental Botany* **61**: 4109–4122.

Pignon CP, Long SP. **2020**. Retrospective analysis of biochemical limitations to photosynthesis in 49 species: C_4 crops appear still adapted to pre-industrial atmospheric [CO_2]. *Plant, Cell & Environment* **43**: 2606–2622.

Pinto H, Sharwood RE, Tissue DT, Ghannoum O. **2014**. Photosynthesis of C_3, C_3–C_4, and C_4 grasses at glacial CO_2. *Journal of Experimental Botany* **65**: 3669–3681.

Pinto H, Tissue DT, Ghannoum O. **2011**. *Panicum milioides* (C_3-C_4) does not have improved water or nitrogen economies relative to C_3 and C_4 congeners exposed to industrial-age climate change. *Journal of Experimental Botany* **62**: 3223–3234.

Pittermann J, Sage RF. **2001**. The response of the high altitude C_4 grass *Muhlenbergia montana* (Nutt.) A.S. Hitchc. to long- and short-term chilling. *Journal of Experimental Botany* **52**: 829–838.

Poorter H, Fiorani F, Pieruschka R, Wojciechowski T, van der Putten WH, Kleyer M, Schurr U, Postma J. **2016**. Pampered inside, pestered outside? Differences and similarities between plants growing in controlled conditions and in the field. *New Phytologist* **212**: 838–855.

Poorter H, Niinemets Ü, Poorter L, Wright IJ, Villar R. **2009**. Causes and consequences of variation in leaf mass per area (LMA): a meta-analysis. *New Phytologist* **182**: 565–588.

R Core Team. **2024**. A language and environment for statistical computing. In: R foundation for statistical computing. https://www.r-project.org/: R v.4.4.1.

Ripley BS, Abraham TI, Osborne CP. **2008**. Consequences of C_4 photosynthesis for the partitioning of growth: a test using C_3 and C_4 subspecies of *Alloteropsis semialata* under nitrogen-limitation. *Journal of Experimental Botany* **59**: 1705–1714.

Ripley BS, Cunniff J, Osborne CP. **2013**. Photosynthetic acclimation and resource use by the C_3 and C_4 subspecies of *Alloteropsis semialata* in low CO_2 atmospheres. *Global Change Biology* **19**: 900–910.

Ripley B, Frole K, Gilbert M. **2010**. Differences in drought sensitivities and photosynthetic limitations between co-occurring C_3 and C_4 (NADP-ME) Panicoid grasses. *Annals of Botany* **105**: 493–503.

Ripley BS, Gilbert ME, Ibrahim DG, Osborne CP. **2007**. Drought constraints on C_4 photosynthesis: stomatal and metabolic limitations in C_3 and C_4 subspecies of *Alloteropsis semialata*. *Journal of Experimental Botany* **58**: 1351–1363.

Sage RF. **2002**. Variation in the k_{cat} of Rubisco in C_3 and C_4 plants and some implications for photosynthetic performance at high and low temperature. *Journal of Experimental Botany* **53**: 609–620.

Sage RF. **2004**. The evolution of C_4 photosynthesis. *New Phytologist* **161**: 341–370.

Sage RF. **2016**. Tracking the evolutionary rise of C_4 metabolism. *Journal of Experimental Botany* **67**: 2919–2922.

Sage RF. **2017**. A portrait of the C_4 photosynthetic family on the 50th anniversary of its discovery: species number, evolutionary lineages, and Hall of Fame. *Journal of Experimental Botany* **68**: e11–e28.

Sage RF, Kubien DS. **2007**. The temperature response of C_3 and C_4 photosynthesis. *Plant, Cell & Environment* **30**: 1086–1106.

Sage RF, Peixoto MM, Sage TL. **2013**. Photosynthesis in Sugarcane. In: Sugarcane: Physiology, Biochemistry, and Functional Biology. 121–154.

Sales CRG, Wang Y, Evers JB, Kromdijk J. **2021**. Improving C_4 photosynthesis to increase productivity under optimal and suboptimal conditions. *Journal of Experimental Botany* **72**: 5942–5960.

Salesse-Smith CE, Sharwood RE, Busch FA, Kromdijk J, Bardal V, Stern DB. **2018**. Overexpression of Rubisco subunits with RAF1 increases Rubisco content in maize. *Nature Plants* **4**: 802–810.

Sharwood RE, Sonawane BV, Ghannoum O. **2014**. Photosynthetic flexibility in maize exposed to salinity and shade. *Journal of Experimental Botany* **65**: 3715–3724.

Smith NG, Dukes JS. **2017**. Short-term acclimation to warmer temperatures accelerates leaf carbon exchange processes across plant types. *Global Change Biology* **23**: 4840–4853.

Smith NG, Dukes JS. **2018**. Drivers of leaf carbon exchange capacity across biomes at the continental scale. *Ecology* **99**: 1610–1620.

Smith NG, Keenan TF, Colin Prentice I, Wang H, Wright IJ, Niinemets Ü, Crous KY, Domingues TF, Guerrieri R, Yoko Ishida F, *et al.* 2019. Global photosynthetic capacity is optimized to the environment. *Ecology Letters* **22**: 506–517.

Soares AS, Driscoll SP, Olmos E, Harbinson J, Arrabaça MC, Foyer CH. **2008**. Adaxial/abaxial specification in the regulation of photosynthesis and stomatal opening with respect to light orientation and growth with CO_2 enrichment in the C_4 species *Paspalum dilatatum*. *New Phytologist* **177**: 186–198.

Soares-Cordeiro AS, Driscoll SP, Arrabaça MC, Foyer CH. **2011**. Dorsoventral variations in dark chilling effects on photosynthesis and stomatal function in *Paspalum dilatatum* leaves. *Journal of Experimental Botany* **62**: 687–699.

Sonawane BV, Sharwood RE, von Caemmerer S, Whitney SM, Ghannoum O. **2017**. Short-term thermal photosynthetic responses of C_4 grasses are independent of the biochemical subtype. *Journal of Experimental Botany* **68**: 5583–5597.

Sonawane BV, Sharwood RE, Whitney S, Ghannoum O. **2018**. Shade compromises the photosynthetic efficiency of NADP-ME less than that of PEP-CK and NAD-ME C_4 grasses. *Journal of Experimental Botany* **69**: 3053–3068.

de Souza AP. **2011**. Photosynthetic mechanisms and source-sink relationship in sugarcane grown in elevated CO_2, University of Sao Paulo.

Still CJ, Berry JA, Collatz GJ, DeFries RS. **2003**. Global distribution of C_3 and C_4 vegetation: carbon cycle implication. *Global Biogeochemical Cycles* **17**: 1–14.

Still CJ, Cotton JM, Griffith DM. **2019**. Assessing earth system model predictions of C_4 grass cover in North America: From the glacial era to the end of this century. *Global Ecology and Biogeography* **28**: 145–157.

Sun W, Ubierna N, Ma J-Y, Cousins AB. **2012**. The influence of light quality on C_4 photosynthesis under steady-state conditions in *Zea mays* and *Miscanthus* × *giganteus*: changes in rates of photosynthesis but not the efficiency of the CO_2 concentrating mechanism. *Plant, Cell & Environment* **35**: 982–993.

Taylor SH, Hulme SP, Rees M, Ripley BS, Ian Woodward F, Osborne CP. **2010**. Ecophysiological traits in C_3 and C_4 grasses: a phylogenetically controlled screening experiment. *New Phytologist* **185**: 780–791.

Tissue DT, Griffin KL, Thomas RB, Strain BR. **1995**. Effects of low and elevated CO_2 on C_3 and C_4 annuals. *Oecologia* **101**: 21–28.

Viechtbauer W. **2010**. Conducting Meta-Analyses in R with the metafor Package. *Journal of Statistical Software* **36**: 1–48.

Vogan PJ, Sage RF. **2012**. Effects of low atmospheric CO_2 and elevated temperature during growth on the gas exchange responses of C_3, C_3–C_4 intermediate, and C_4 species from three evolutionary lineages of C_4 photosynthesis. *Oecologia* **169**: 341–352.

Wang Y, Bräutigam A, Weber APM, Zhu X-G. **2014**. Three distinct biochemical subtypes of C_4 photosynthesis? A modelling analysis. *Journal of Experimental Botany* **65**: 3567–3578.

Wang F, Gao J, Yong JWH, Wang Q, Ma J, He X. **2020**. Higher atmospheric CO_2 levels favor C_3 plants over C_4 plants in utilizing ammonium as a nitrogen source. *Frontiers in Plant Science* **11**: 537443.

Wang Z, Kang S, Jensen CR, Liu F. **2012**. Alternate partial root-zone irrigation reduces bundle-sheath cell leakage to CO_2 and enhances photosynthetic capacity in maize leaves. *Journal of Experimental Botany* **63**: 1145–1153.

Wang D, Portis AR Jr, Moose SP, Long SP. **2008**. Cool C_4 photosynthesis: Pyruvate P_i dikinase expression and activity corresponds to the exceptional cold tolerance of carbon assimilation in *Miscanthus × giganteus*. *Plant Physiology* **148**: 557–567.

Ward DA. **1987**. The temperature acclimation of photosynthetic responses to CO_2 in *Zea mays* and its relationship to the activities of photosynthetic enzymes and the CO_2-concentrating mechanism of C_4 photosynthesis. *Plant, Cell & Environment* **10**: 407–41.

Wasilewska-Dębowska W, Zienkiewicz M, Drozak A. **2022**. How light reactions of photosynthesis in C_4 plants are optimized and protected under high light conditions. *International Journal of Molecular Sciences* **23**: 3626.

Way DA, Yamori W. **2014**. Thermal acclimation of photosynthesis: on the importance of adjusting our definitions and accounting for thermal acclimation of respiration. *Photosynthesis Research* **119**: 89–100.

Wickham H. **2016**. *ggplot2: Elegant Graphics for Data Analysis*. New York: Springer-Verlag.

Wong SC. **1979**. Elevated atmospheric partial pressure of CO_2 and plant growth. I. Interactions of nitrogen nutrition and photosynthetic capacity in C_3 and C_4 plants. *Oecologia* **44**: 68–74.

Wu A, Truong SH, McCormick R, van Oosterom EJ, Messina CD, Cooper M, Hammer GL. **2024**. Contrasting leaf-scale photosynthetic low-light response and its temperature dependency are key to differences in crop-scale radiation use efficiency. *New Phytologist* **241**: 2435–2447.

Xu Z, Shimizu H, Ito S, Yagasaki Y, Zou C, Zhou G, Zheng Y. **2014**. Effects of elevated CO_2, warming and precipitation change on plant growth, photosynthesis and peroxidation in dominant species from North China grassland. *Planta* **239**: 421–435.

Yamori W, Hikosaka K, Way DA. **2014**. Temperature response of photosynthesis in C_3, C_4, and CAM plants: temperature acclimation and temperature adaptation. *Photosynthesis Research* **119**: 101–117.

Tables

Table 1. Results of multivariate linear mixed-effects models testing the response of V_{pmaxA} and A_{max} against fixed effects of species-specific traits and experimental conditions (see main text for more details). Effect size denotes the number of studies, while the sample size is the number of V_{pmaxA} or A_{max} data points. Model's marginal R^2 reflects the variance explained by fixed effects only, whereas conditional R^2 considers the variance explained by both fixed and random effects. Bold text indicates statistical significance. Significant codes: *, $P < 0.05$; **, $P < 0.01$; ***, $P < 0.001$. Continuous variables (i.e. mean T_{max}, growth CO_2, T_{leaf} and *PPFD*) were mean-centred before the analysis. SE = standard error. Lower and high CI: lower and upper 95% confidence intervals.

Fixed effects	$\boldsymbol{V}_{\mathbf{pmaxA}}$					$\boldsymbol{A}_{\mathbf{max}}$				
	Estimate	SE	Lower CI	Higher CI	*P* value	Estimate	SE	Lower CI	Higher CI	*P* value
C_4 subtype	-1.299	7.716	-16.470	13.873	0.969	-1.339	3.363	-7.960	5.282	0.727
Growth form	0.270	8.272	-15.996	16.535	0.196	-15.091	11.082	-37.636	7.455	0.295
Growth location	-15.190	5.154	-25.747	-4.634	**0.005****	-6.676	2.651	-12.295	-1.057	**0.018***
Mean T_{max}	-2.549	1.362	-5.228	0.130	**0.001****	0.367	0.754	-1.117	1.851	**0.001****
Growth CO_2	-0.018	0.012	-0.042	0.006	0.138	-0.003	0.009	-0.021	0.016	0.761
T_{leaf}	3.580	0.849	1.910	5.250	**< 0.0001*****	2.406	0.476	1.468	3.343	**< 0.0001*****
PPFD	0.014	0.002	0.010	0.018	**< 0.0001*****	0.010	0.001	0.008	0.013	**< 0.0001*****
C_4 subtype × T_{leaf}	0.544	0.519	-0.477	1.565	0.504	0.187	0.261	-0.327	0.700	0.761
C_4 subtype × Mean T_{max}	-0.413	2.268	-4.873	4.047	0.840	-0.943	1.188	-3.283	1.396	0.642
C_4 subtype × *PPFD*	-0.001	0.005	-0.010	0.008	0.674	0.002	0.003	-0.003	0.007	0.750
Growth form × T_{leaf}	-1.412	0.982	-3.342	0.518	0.146	3.590	2.519	-1.368	8.549	0.219
Growth form × Mean T_{max}	3.477	2.132	-0.890	7.845	0.099	0.148	1.207	-2.410	2.707	0.781
Growth form × *PPFD*	0.004	0.008	0.631	-0.012	0.645	-0.023	0.019	-0.066	0.007	0.143
T_{leaf} × Mean T_{max}	0.013	0.036	-0.058	0.083	0.724	-0.043	0.020	-0.082	-0.004	**0.033***
Species group	8.209	6.740	-5.385	21.802	0.230	3.467	2.381	-1.376	8.311	0.155
Overall model statistics	$\boldsymbol{V}_{\mathbf{pmaxA}}$					$\boldsymbol{A}_{\mathbf{max}}$				
Effect size/sample size	49/401					37/297				

Marginal R^2	0.51	0.47
Conditional R^2	0.83	0.75

Figures

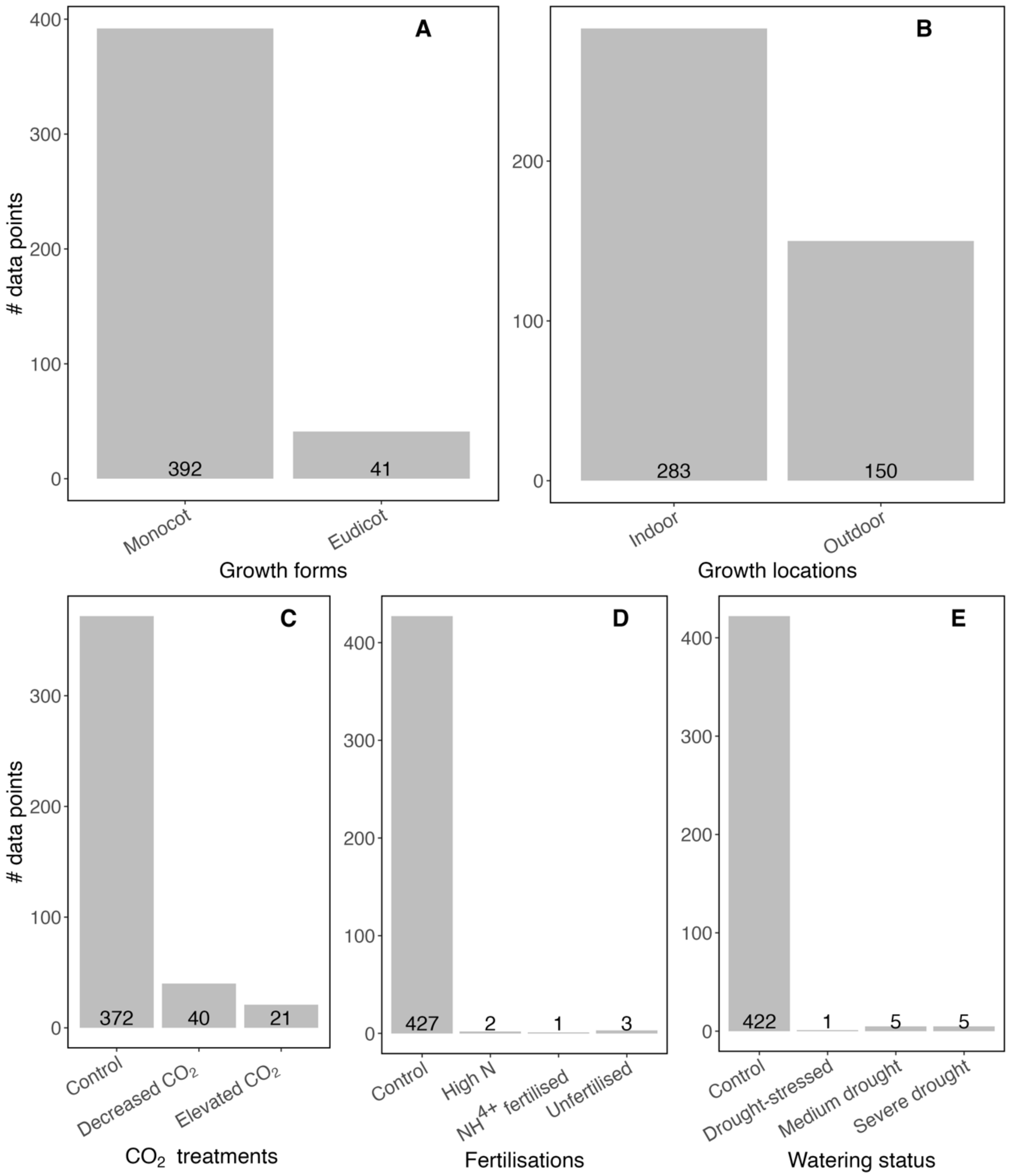

Figure 1. A summary of data points (by groups) based on (A) growth forms, (B) locations, (C) CO_2 treatments, (D) fertilisation treatments and (E) watering status. Decreased and elevated CO_2 treatments consist of measurements made on plants with a growth CO_2 concentration of < 400 ppm and > 400 ppm, respectively. See Materials and Methods for more information.

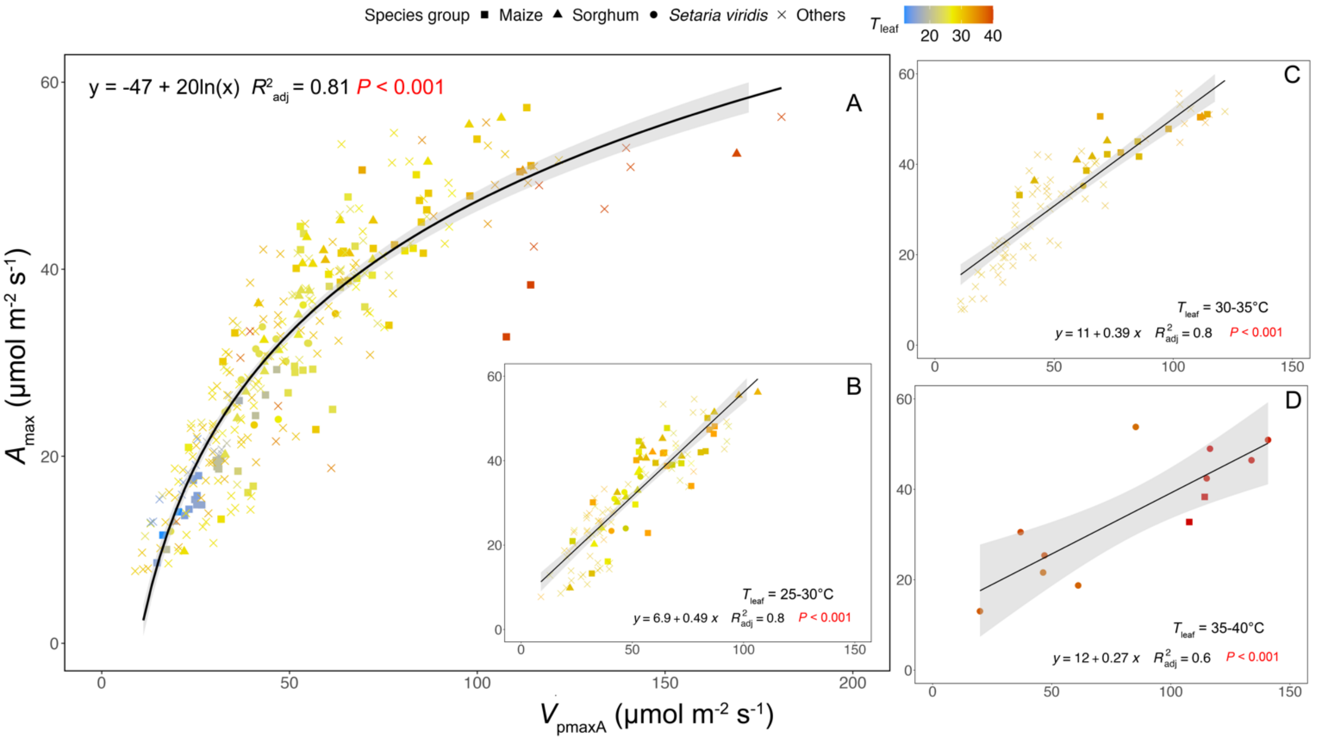

Figure 2. Correlation of A_{max} versus V_{pmaxA} estimated from data collected from a range of species measured at various growth and measuring conditions. Point shapes reflect important species groups and colours denote measurement temperature (T_{leaf}). (A) All available A_{max}-V_{pmaxA} data; (B–D) data subsets measured at 25–30°C, 30–35°C, and 35–40°C, respectively. Equation, adjusted R^2 values and P values of individual fits are shown in each panel.

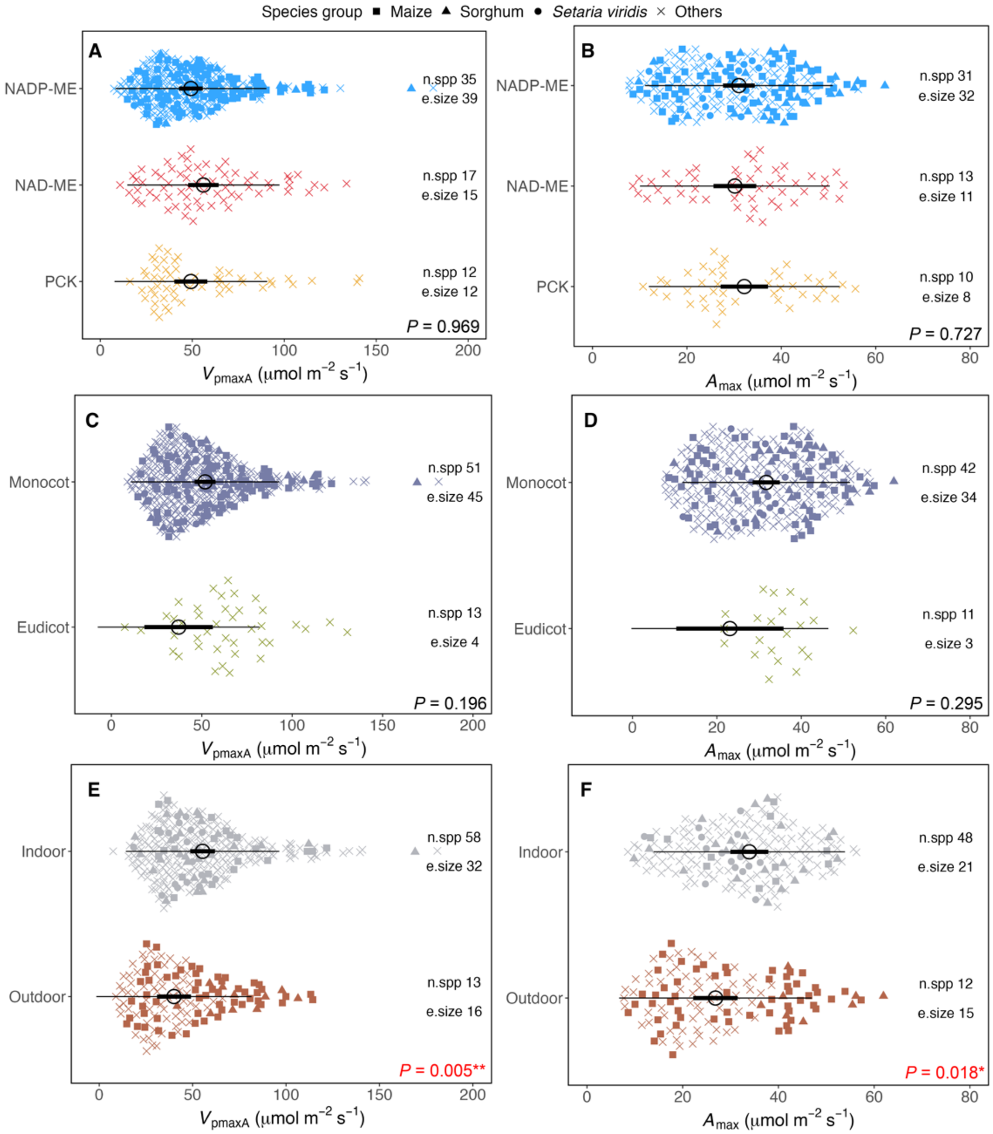

Figure 3. V_{pmaxA} and A_{max} plotted by C$_4$ biochemical subtypes (A and B, respectively), growth forms (C and D, respectively) and growth locations (E and F, respectively). Data presented here are a mixture of measurements done at various growth and measuring temperatures and irradiance. Raw data points are plotted as coloured symbols, with different symbol shapes reflecting important species groups. Model-predicted marginal means and intervals are shown as a horizontal line. On this line, black circles indicate model-predicted meta-analytic means of V_{pmaxA} or A_{max}, thick bars are 95% confidence intervals and thin bars are 95% prediction intervals. On the right-hand side of each panel, the number of unique species per category (n.spp) and the number of individual studies (e.size) are indicated. P values are indicated in each panel (see Table 1). Significant codes: *, $P < 0.05$; **, $P < 0.01$; ***, $P < 0.001$.

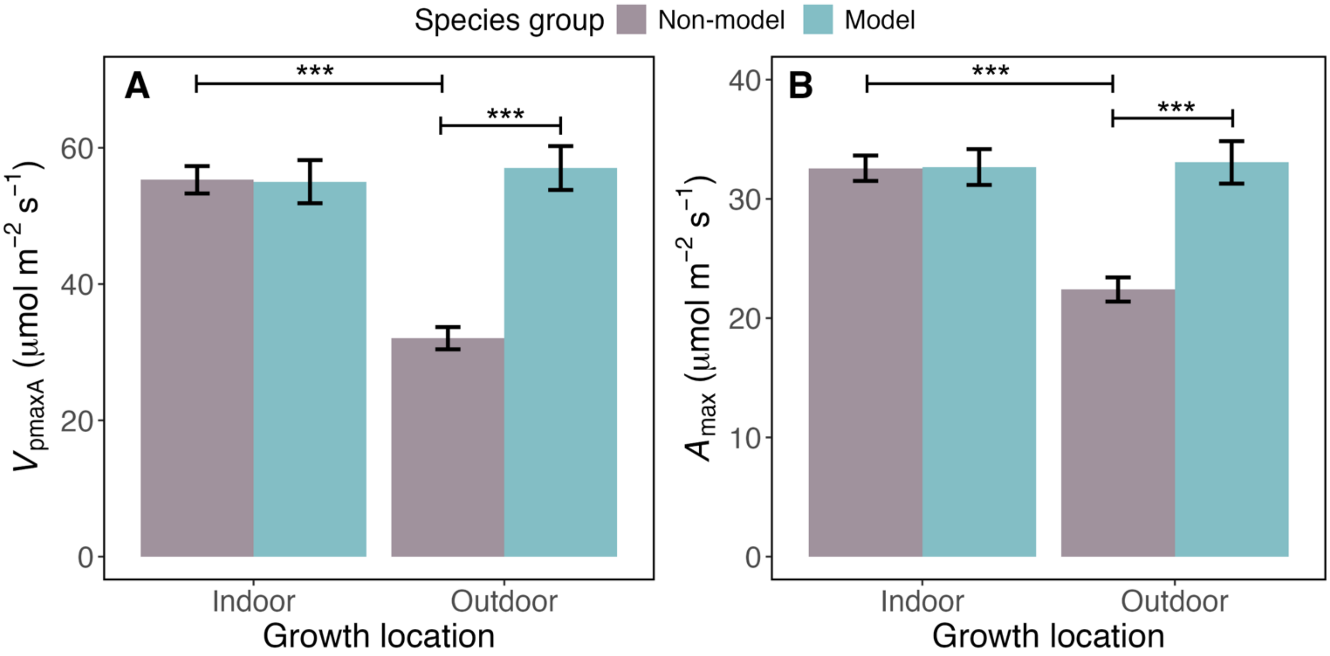

Figure 4. Comparison between V_{pmaxA} and A_{max} (mean ± SE) with growth location coloured by species group (C_4 non-model species versus model species). A linear mixed-effect model was conducted to examine V_{pmaxA} and A_{max} between two species groups at a location, or within a species group at both locations. Statistical results of comparisons are denoted with horizontal lines (i.e. the two bars at the beginning and the end of a horizontal line are compared) and asterisks indicate statistical significance (*, $P < 0.05$; **, $P < 0.01$; ***, $P < 0.001$).

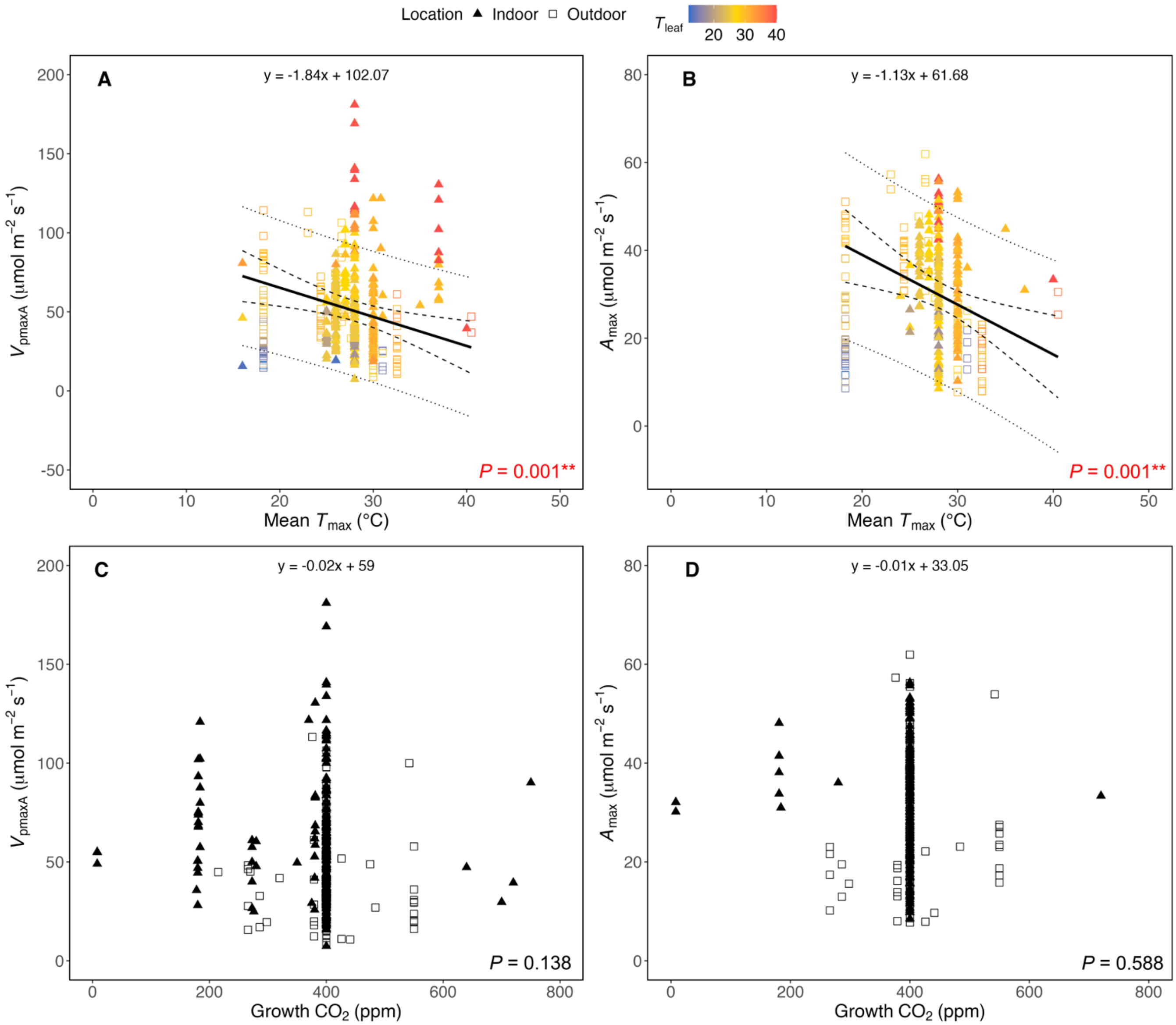

Figure 5. Relationships between V_{pmaxA} and A_{max} with mean T_{max} (A and B, respectively) and growth $\mathrm{CO_2}$ levels (C and D, respectively). Data points in (A) and (B) are coloured in gradient by the measurement temperature (T_{leaf}), and the shapes of data points in all panels reflect the growth location (i.e. indoor vs. outdoor). Solid lines represent model-predicted values of V_{pmaxA} or A_{max} at a given mean T_{max} or $\mathrm{CO_2}$ level (equations are shown at the top of each panel), dashed lines indicate 95% confidence intervals, and dotted lines show 95% prediction intervals. *P* values of the multivariate linear mixed-effects models are indicated. Significant codes: *, $P < 0.05$; **, $P < 0.01$; ***, $P < 0.001$.

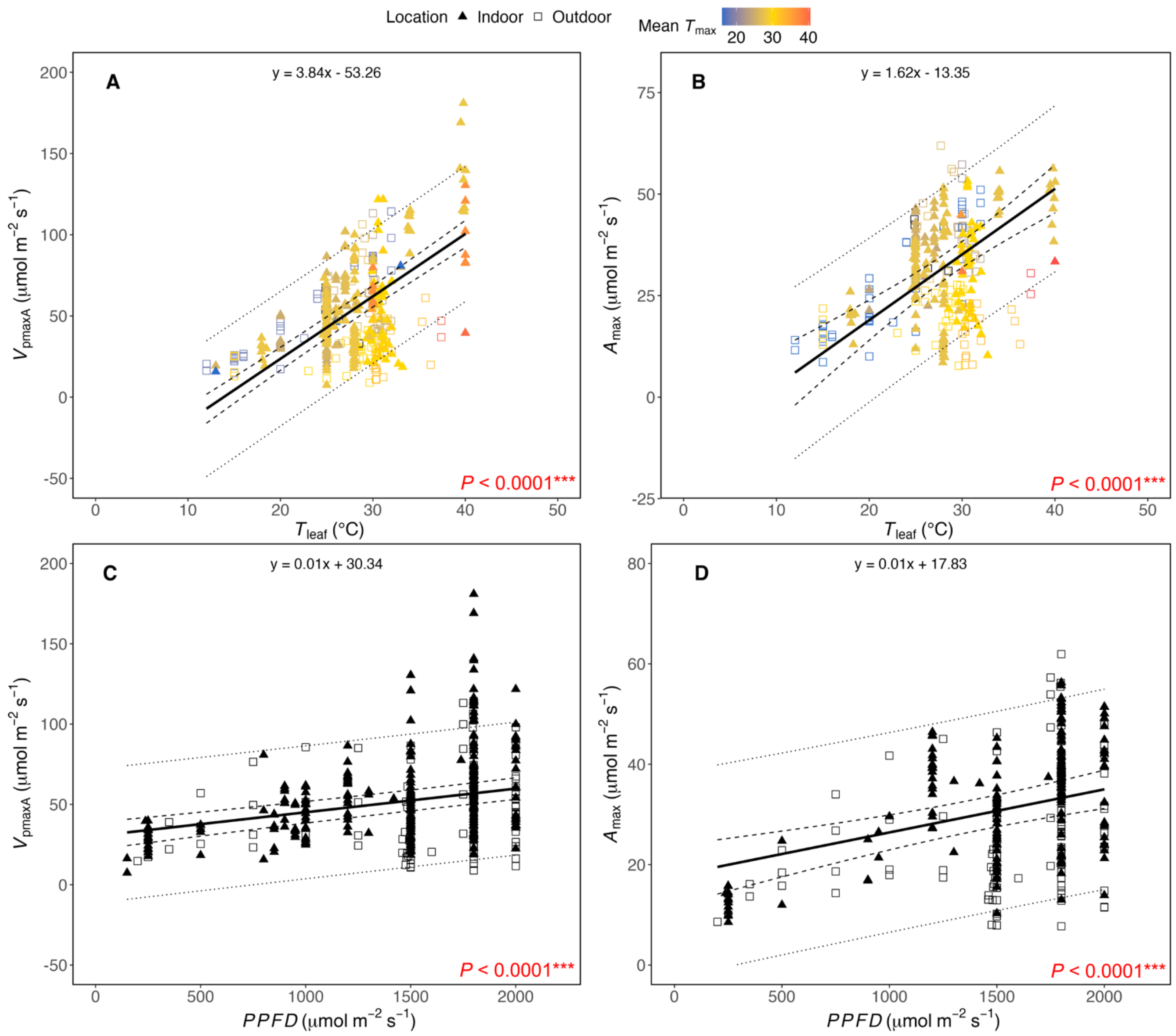

Figure 6. Relationships between V_{pmaxA} and $A_{\max}$ with T_{leaf} (A and B, respectively) and *PPFD* (C and D, respectively). Data points in (A) and (B) are coloured by the mean maximum growth temperature (mean $T_{\max}$), and the shapes of data points in all panels reflect the growth location (i.e. indoor vs. outdoor). Solid lines represent model-predicted values of V_{pmaxA} or $A_{\max}$ at a given T_{leaf} or *PPFD* (equations are shown at the top of each panel), dashed lines indicate 95% confidence intervals, and dotted lines show 95% prediction intervals. P values of the multivariate linear mixed-effects models are indicated. Significant codes: *, $P < 0.05$; **, $P < 0.01$; ***, $P < 0.001$.

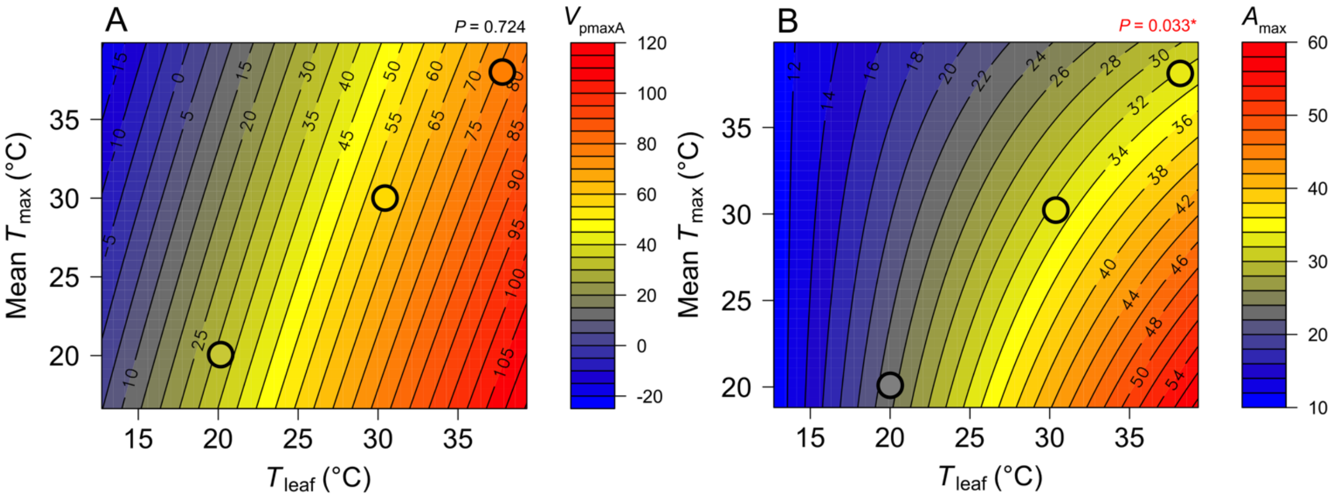

Figure 7. Contour plots illustrating the model-predicted responses of V_{pmaxA} and A_{max} (μmol m^{-2} s^{-1}) to T_{leaf} and mean T_{max}. P values of linear mixed-effects model testing the interaction between T_{leaf} and mean T_{max} are indicated (see Table 1). Black circle represent comparisons of V_{pmaxA} and A_{max} at the same mean T_{max} and T_{leaf} of 20, 30 and 38°C, with the colour gradient reflecting changes in V_{pmaxA} and A_{max} (see the colour legend on the right-hand side of each panel). Significant codes: *, $P < 0.05$; **, $P < 0.01$; ***, $P < 0.001$.

Supporting Information

Table S1. Results of multivariate linear mixed-effects models testing the response of V_{pmaxA} and A_{max} against species-specific traits and experimental conditions for **data with *PPFD* > 1000 μmol photon m^{-2} s^{-1}**. See Table 1 and main text for more details. Effect size denotes the number of studies, while the sample size is the number of V_{pmaxA} or A_{max} data points. Model's marginal R^2 reflects the variance explained by fixed factors only, whereas conditional R^2 considers the variance explained by both fixed and random factors. Bold text indicates statistical significance. Significant codes: *, $P < 0.05$; **, $P < 0.01$; ***, $P < 0.001$.

	V_{pmaxA}	A_{max}
Fixed effects		
C_4 subtype	0.764	0.864
Growth form	0.294	0.760
Growth location	**0.013***	**0.030***
Mean T_{max}	**0.002****	**0.003****
Growth CO_2	0.097	0.542
T_{leaf}	**< 0.0001*****	**< 0.0001*****
PPFD	0.119	0.061
C_4 subtype × T_{leaf}	0.795	0.702
C_4 subtype × Mean T_{max}	0.960	0.744
C_4 subtype × *PPFD*	0.704	0.795
Growth form × T_{leaf}	0.219	0.263
Growth form × Mean T_{max}	0.625	0.692
Growth form × *PPFD*	0.097	0.521
T_{leaf} × Mean T_{max}	0.278	**0.002****
Species group	0.179	0.162
Overall model statistics		
Effect size/sample size	43/317	34/261
Marginal R^2	0.50	0.41
Conditional R^2	0.80	0.72

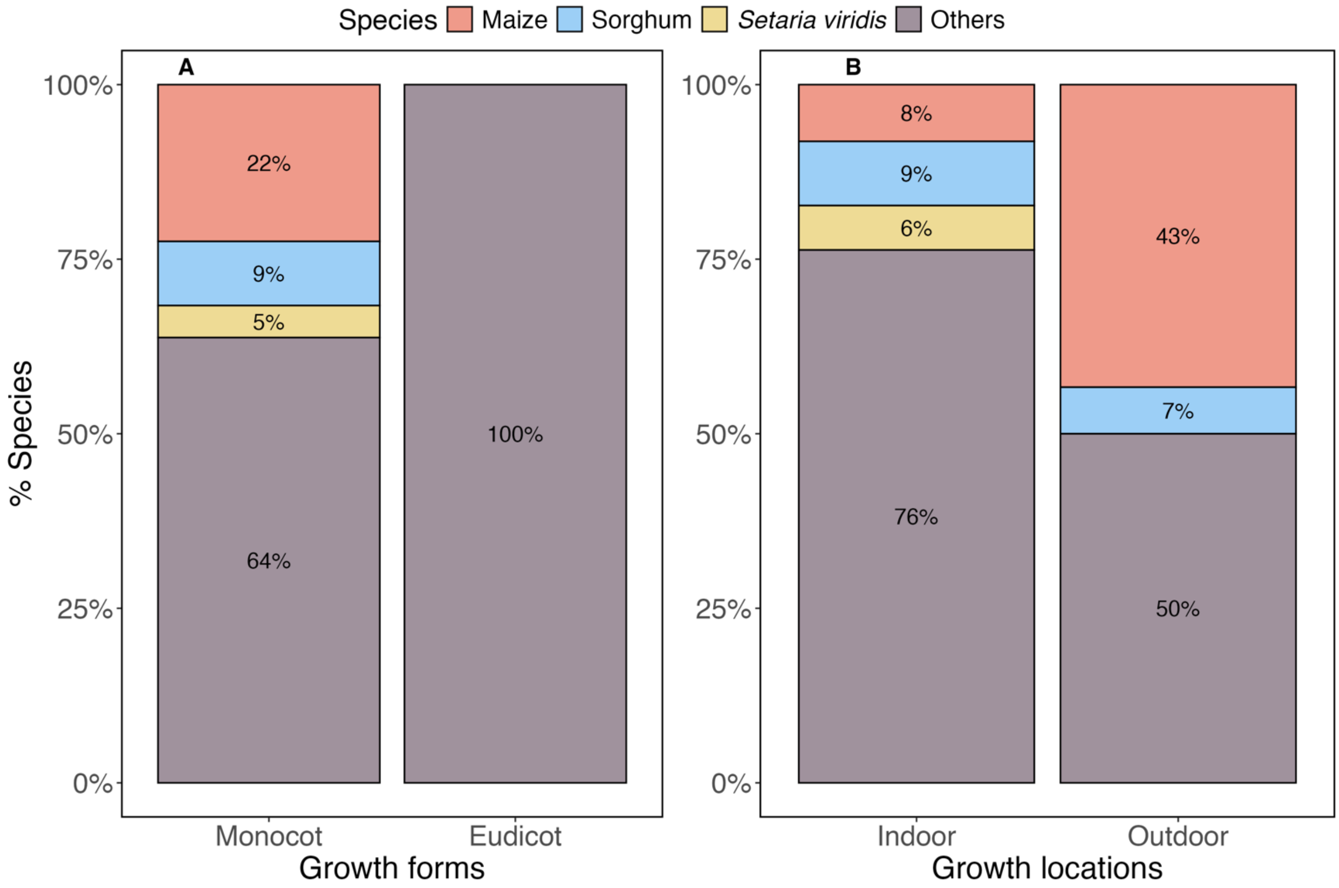

Figure S1. Species distribution within the categories of (A) growth forms and (B) growth locations. The top three measured species (maize, sorghum and *Setaria viridis*) are labelled explicitly, whereas all other species are shown as "Others". Detailed information on species is available in Supplementary Datasets S1 and S2.

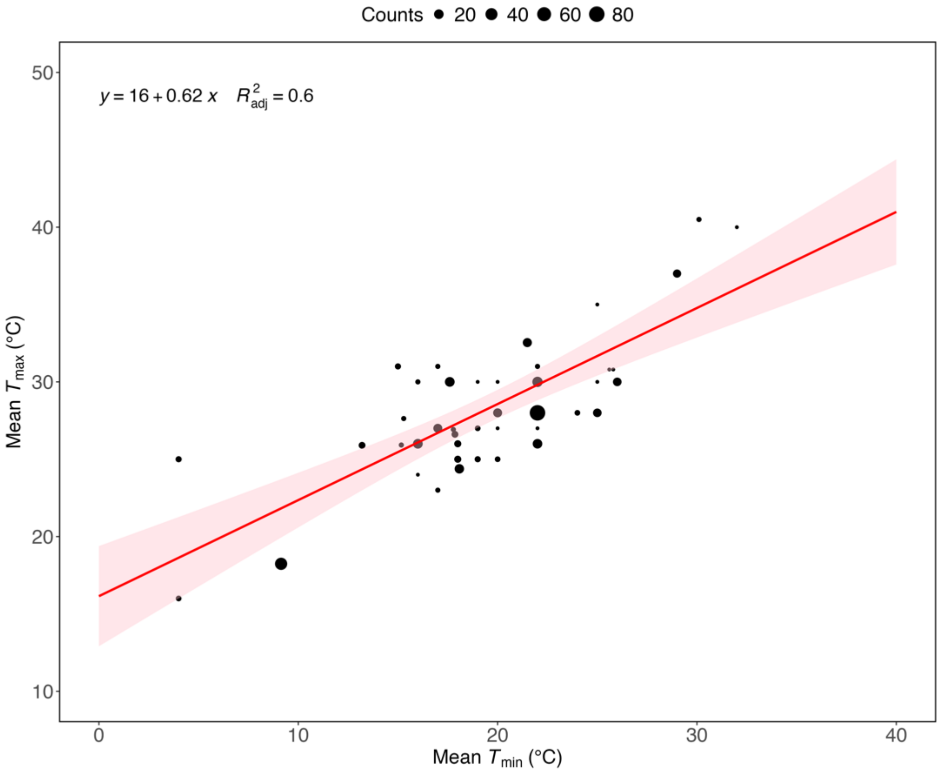

Figure S2. Correlation of mean $T_{\max}$ and $T_{\min}$ (°C). The size of the dots reflects the number of A/C_{i} curve groups. See Supplementary Dataset S1 for more details.

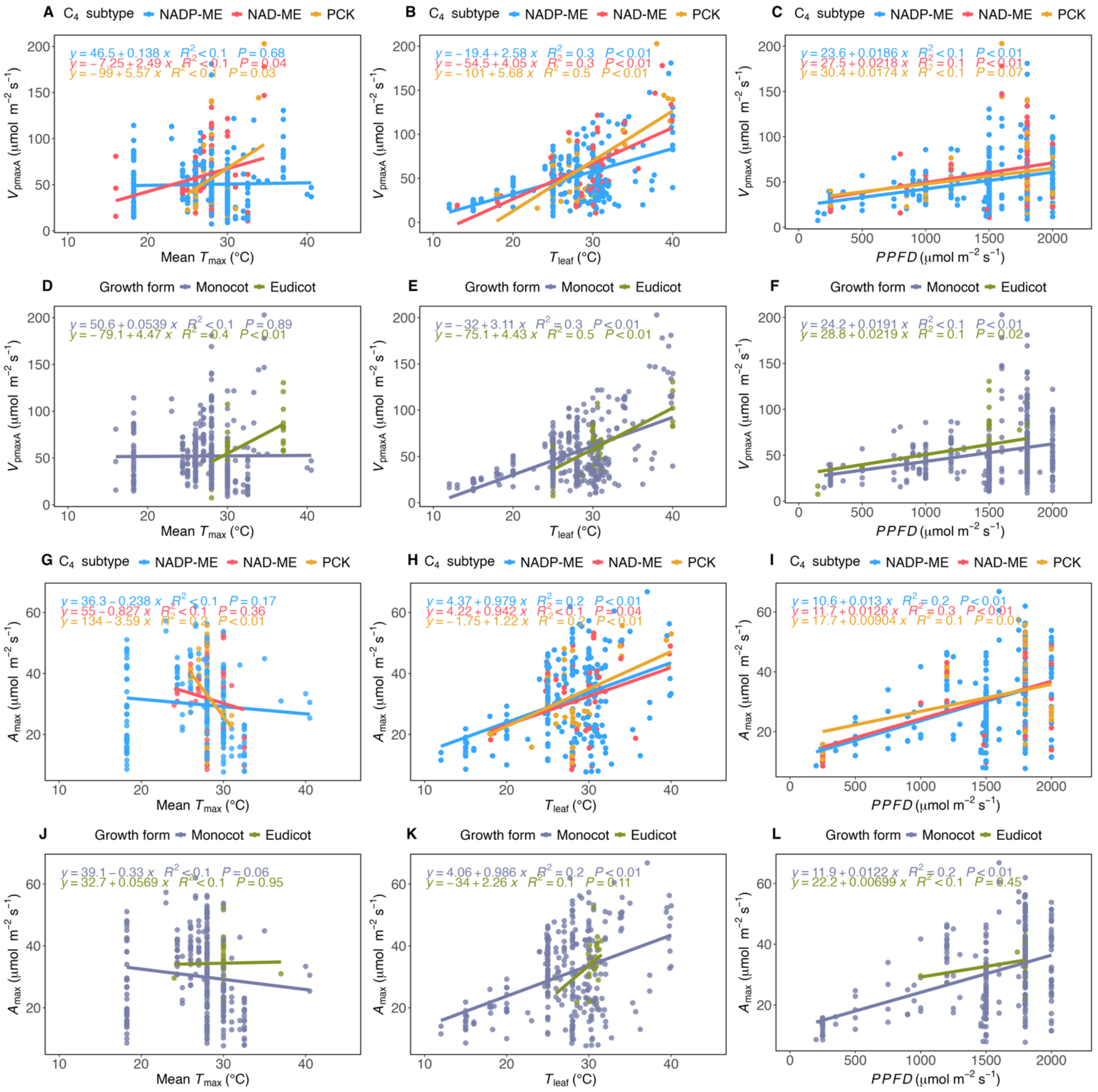

Figure S3. Data distribution of V_{pmaxA} and $A_{\max}$ in categories of C_4 subtypes and growth forms over T_{leaf}, mean $T_{\max}$ and *PPFD*. Linear regression is fitted to each category within each panel, with equations, adjusted R^2 and P values being shown.

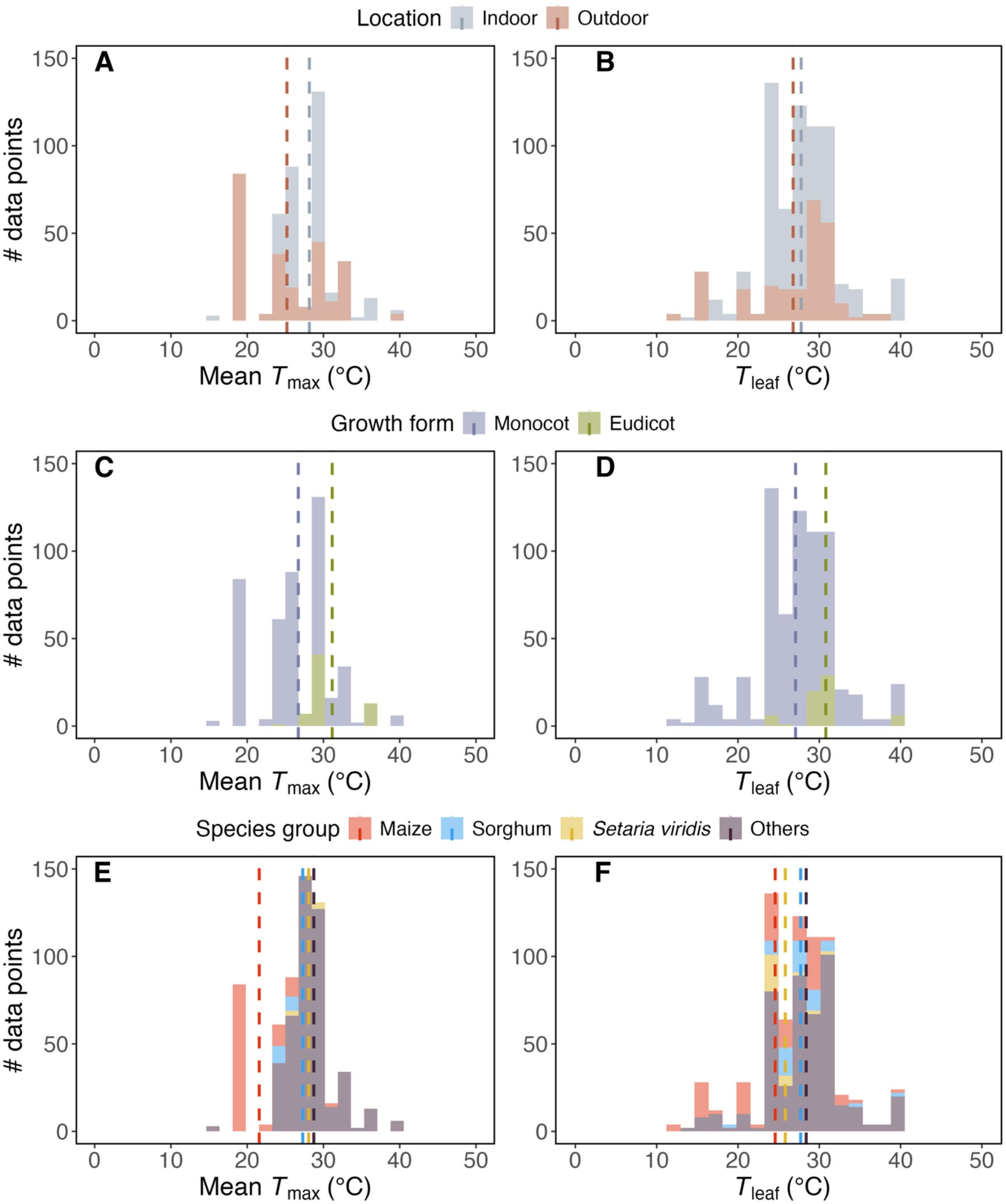

Figure S4. Histograms describing the data distribution across the spectrum of mean T_{max} and T_{leaf} for growth location (A & B), growth form (C & D) and important species group (E & F). Dash lines indicate the average values of mean T_{max} and T_{leaf} across plants grouped by different traits.

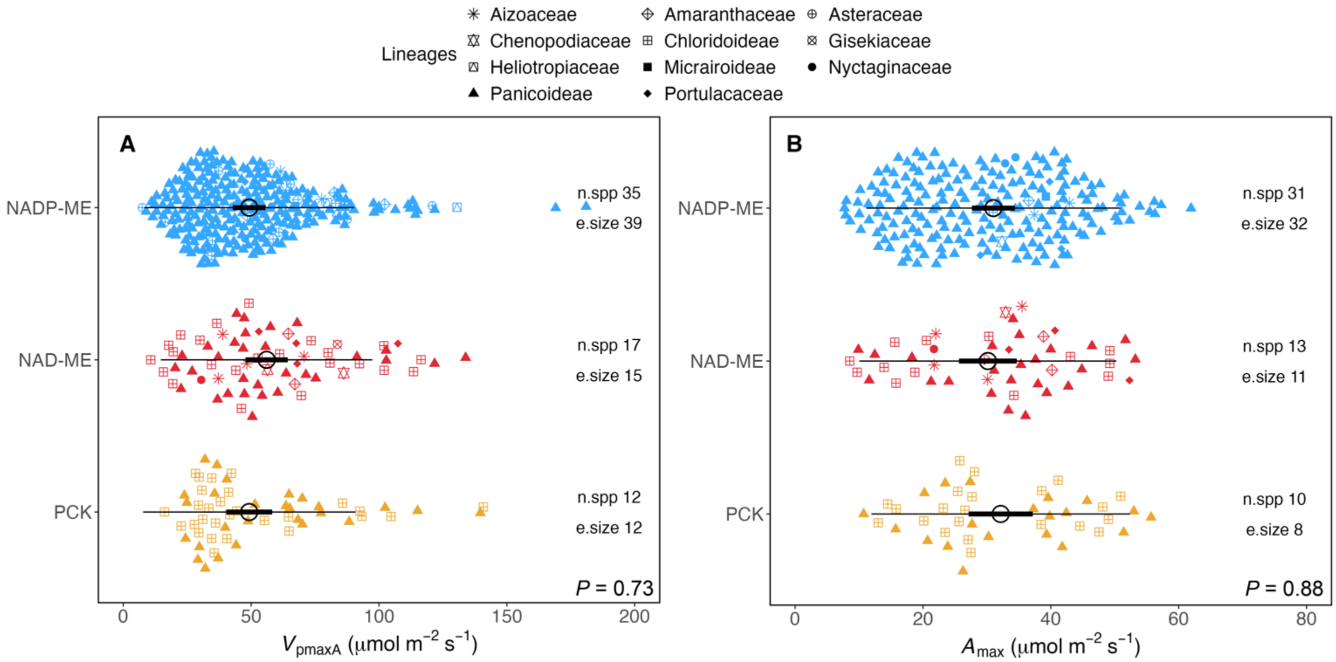

Figure S5. V_{pmaxA} and A_{max} plotted by C$_4$ biochemical subtypes (A and B, respectively). Data presented here are a mixture of measurements done at various growth and measuring temperatures and irradiance. Raw data points are plotted as coloured symbols, with different symbol shapes reflecting lineages. Model-predicted marginal means and intervals are shown as a horizontal line. On this line, black circles indicate model-predicted meta-analytic means of V_{pmaxA} or A_{max}, thick bars are 95% confidence intervals and thin bars are 95% prediction intervals. On the right-hand side of each panel, the number of unique species per category (n.spp) and the number of individual studies (e.size) are indicated. *P* values of a multivariate mixed effect model indicating the effect of lineages on V_{pmaxA} and A_{max} are shown on each panel. Significant codes: *, $P < 0.05$; **, $P < 0.01$; ***, $P < 0.001$.

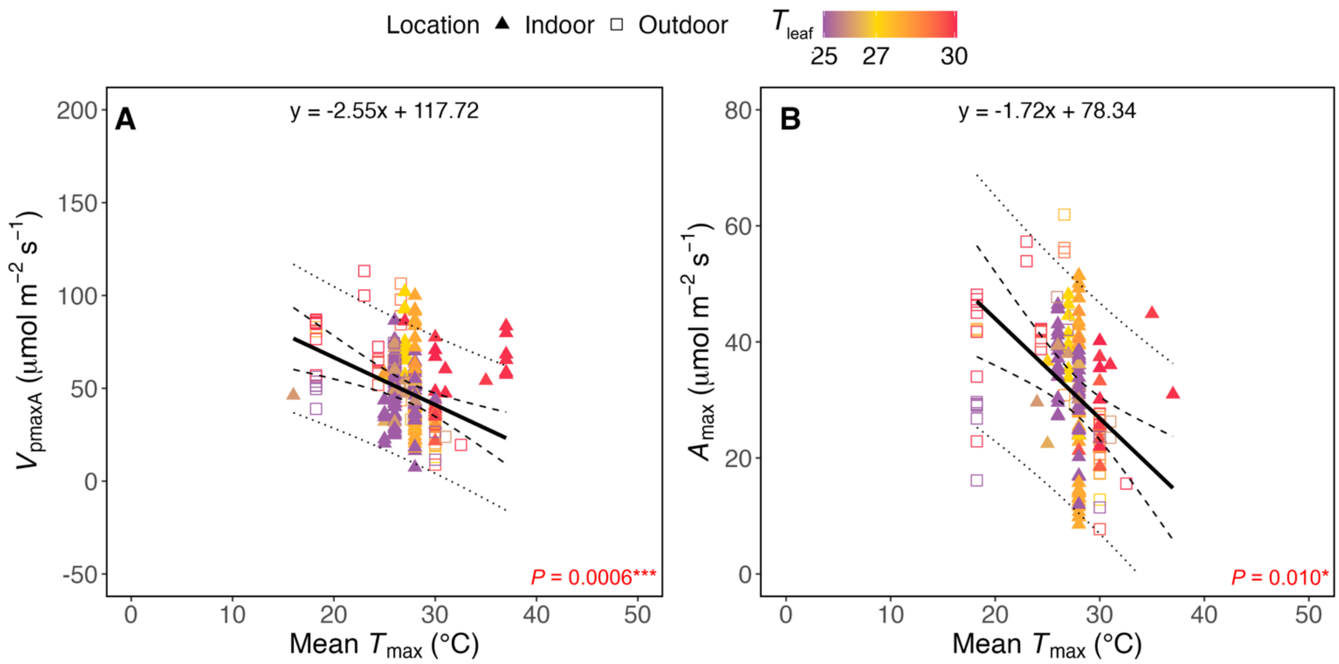

Figure S6. Relationships between V_{pmaxA} and A_{max} with mean T_{max} (A and B, respectively) for measurements done at T_{leaf} between 25 and 30°C. Data presented here are a mixture of measurements done at various *PPFD*. Data points are coloured in gradient by T_{leaf}, the shapes of data points in all panels reflect the growth location (i.e. indoor vs. outdoor). Solid lines represent model-predicted values of V_{pmaxA} or A_{max} at a given T_{leaf} or *PPFD* (equations are shown at the top of each panel), dashed lines indicate 95% confidence intervals, and dotted lines show 95% prediction intervals. *P* values of the multivariate linear mixed-effects models are indicated. Significant codes: *, $P < 0.05$; **, $P < 0.01$; ***, $P < 0.001$.

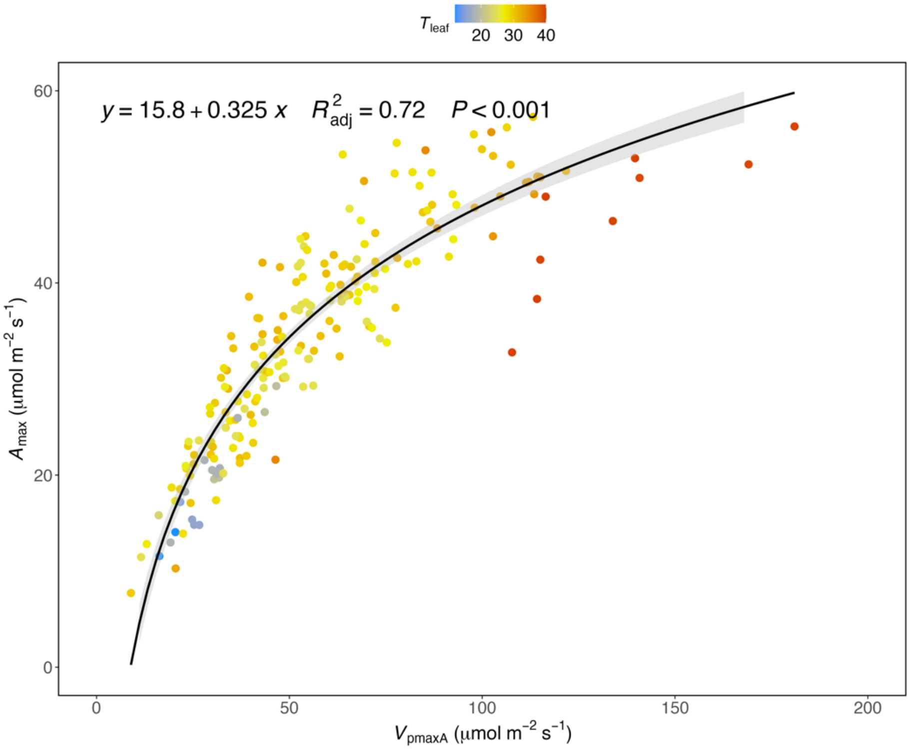

Figure S7. Correlation of A_{max} versus V_{pmaxA} estimated from data with $PPFD > 1{,}500$ μmol photon m^{-2} s^{-1}, coloured by T_{leaf}.